Nye County Nuclear Waste Repository Project Office Independent Scientific Investigations Program: Preliminary Evaluation of a Modified Conceptual Design of a Naturally-Ventilated Repository

Prepared for:
Nye County Department of Natural Resources and Federal Facilities,
Nuclear Waste Repository Project Office, Oversight

Prepared by:
Multimedia Environmental Technology, Inc.

February 2002

NWRPO-2002-02

EXECUTIVE SUMMARY

The Nye County Nuclear Waste Repository Project Office has conducted several preliminary studies to evaluate the feasibility of a naturally-ventilated nuclear waste repository at Yucca Mountain, Nevada. This preliminary work, which suggested that natural ventilation could maintain cool and dry conditions within the proposed repository indefinitely, is summarized in NWRPO (1998). In these earlier studies, the ventilation drifts and shafts were considered to remain open to the atmosphere. This requirement was criticized by Yucca Mountain scientists because of concerns about the potential for human intrusion and the stability of the ventilation drifts and shafts. The following report presents an alternative conceptual design and preliminary performance evaluations for a permanently-ventilated repository (PVR) that is believed to address these concerns, as well as maintain a cool and dry repository.

The PVR design provides a network of stable pathways for natural ventilation and minimizes the contact of the ventilation air with the waste packages. In this design, an essentially separate network of tunnels, drifts, and shafts will be backfilled with highly-porous and permeable rubble to provide ventilation during and after the pre-closure period. It is believed that the rubble backfill will provide stability without blocking the air-flow through the passages and at the same time help prevent human intrusion. This design also requires that the waste emplacement boreholes be directly ventilated during the pre-closure period to aid in cooling waste packages when they are producing the maximum amount of heat. Following the pre-closure period, the waste emplacement boreholes will be sealed off from the ventilation system.

Major components of the PVR include intake drifts that will supply air from lower elevations on the east flank of Yucca Mountain, cross drifts that will pass this air through the repository removing heat and moisture, exhaust shafts that will provide exits for this warm and moist air, and chimneys on the west flank of Yucca Mountain that will enhance the efficiency of air flow by increasing the differential elevation between the intake and exit points in the system. Additional optional components, such as a drainage system, that are intended to prolong the efficient operation of the ventilation system are also briefly described in this report.

Two-dimensional numerical modeling results are used to compare the performance of two main configurations of the emplacement and ventilation system. The first, or baseline configuration (Configuration A), considers rubble-filled ventilation drifts spaced 70 m apart with five to six waste emplacement boreholes between the drifts. The alternative configuration (Configuration B) consists of rubble-filled drifts spaced 30 m apart with only two waste emplacement boreholes between the drifts. To ensure the stability of underground openings, at least a 10-m spacing was maintained between all boreholes and drifts. Both configurations, with fully-packed waste emplacement boreholes (with waste packages placed end to end), will fit in an area of less than 1,000 m by 1,000 m (1×10^6 m^2, or 247 acres). In the analyses presented in this report, the heat loading is reduced by increasing the spacing of the waste packages in the waste emplacement boreholes.

Several experimental mesh configurations were used to test the baseline and alternative configurations proposed for the PVR. Various heat-loading scenarios were used to simulate waste emplacement. The purpose of these experimental setups was to evaluate the best

combination of ventilation drifts and emplacement boreholes to maintain the temperature of the host rock below boiling and minimize the required footprint for the disposal area.

The results of the preliminary simulations demonstrated that reasonably low temperatures may be achieved with significant reduction in the acreage requirements by increasing the number of the ventilation drifts, reducing the number of waste-emplacement boreholes between drifts, and using pre-closure direct ventilation of the waste emplacement boreholes. For example, preliminary analyses indicated that over a 250-yr. period of pre-closure ventilation and using a footprint of about 500 acres, natural ventilation maintains the temperature of the host rock below 55°C.

Additional in-depth analyses need to be conducted to evaluate the feasibility of different configurations of the PVR design in more detail. These analyses should include two- and three-dimensional modeling to evaluate numerous parameters and variations of the PVR design in more detail. For example, further evaluations should be performed to determine the importance of heat and moisture transfer coefficients (eddy diffusivity) between rock and ventilation drifts. In addition, the size, number, and location of the intake drifts, exhaust shafts, and chimneys must be determined. Rubble properties also need to be evaluated in more detail. Moreover, the role fractures play in heat and moisture transfer must be fully evaluated. It is possible that by incorporating fractures into the model, the convective heat transport may reduce the temperature significantly. Finally, other important unresolved issues must be addressed, including gaseous radionuclide migration, long-term maintenance of rubble permeability, and the stability of exposed entrances and exits of the ventilation system.

CONTENTS

FIGURES

FIGURES (continued)

TABLES

APPENDIX

INTENTIONALLY LEFT BLANK

ACRONYMS AND ABBREVIATIONS

A-TOUGH2	Atmospheric TOUGH2
CHnw	Calico Hills nonwelded
DOE	U.S. Department of Energy
HTOM	high temperature operating mode
LTOM	low temperature operating mode
MTU	metric tons of uranium
PTn	Paintbrush Tuff nonwelded
PVR	permanently-ventilated repository
TCw	Tiva Canyon welded
TSw	Topopah Spring welded

INTENTIONALLY LEFT BLANK

1.0 MODIFIED CONCEPTUAL DESIGN OF A NATURALLY-VENTILATED REPOSITORY

1.1 INTRODUCTION

Nye County, after performing a series of analyses and calculations, recommended a conceptual design for a naturally-ventilated repository at Yucca Mountain (NWRPO, 1996). In a 1996 and 1998 patent, Montazer introduced the idea of a ventilated repository design in which the host rock would be maintained at relatively low temperatures and dry conditions[1] (Montazer, 1996 and 1998). It was assumed in both the 1996 and 1998 designs that the repository area was to remain open indefinitely with no backfill to promote natural ventilation.

The main disadvantages of the open repository concept are the potential instability of the underground openings and the difficulty in preventing human intrusion. Subsequently, several recommendations for blocking the entrance to the repository were suggested by Nye County to minimize human intrusion. These recommendations included the installation of multiple steel bar grids combined with a coarse wire mesh system. None of these closure concepts were supported by repository design engineers or regulatory agencies concerned with Yucca Mountain.

The Nuclear Regulatory Commission's final licensing regulations require at least 50 yr. of pre-closure monitoring in an open repository and permit a longer period of retrievability (pre-closure period) if required (10 CFR 63; NRC, 2001). The U.S. Department of Energy (DOE), in its latest science and engineering report, considered extending the pre-closure time period to 300 yr. as one of its alternative design options (DOE, 2001a). DOE also considered the option of keeping the repository open to monitor its performance for an indefinite period of time. This option would provide future generations an opportunity to retrieve the waste if a beneficial use was found and/or a safer disposal method was identified.

In this same report, DOE recommended two basic designs for the repository: LTOM (low temperature operating mode) and HTOM (high temperature operating mode). HTOM is designed to allow the waste packages to approach temperatures of over 96ºC, which is above the boiling point of water at the elevation of Yucca Mountain. The LTOM is designed to maintain the temperature of the waste packages below 85°C. The main disadvantage of the HTOM is the high temperature of the host rock. These disadvantages were pointed out by the Nuclear Waste Technical Review Board and other expert panels, who emphasized that the state of the art of thermomechanical hydrological science is in its infancy and the coupled thermal-hydrological-mechanical-chemical processes involved are complex and difficult to simulate. For example, existing numerical codes that are designed to simulate these coupled processes have not been successfully tested for such a large volume of rock. Furthermore, experimental data, against which these codes have been validated, are available only for relatively short periods. Although

[1] "Dry conditions" are considered in this report to be moisture conditions in the host rock below which water is substantially immobile. For water to be substantially immobile, a limit is arbitrarily defined where the effective permeability of the rock is at least 10,000 times less than its water-saturated permeability; that is, the relative permeability is less than $1x10^{-4}$.

analog sites have been used for validation of portions of these codes, the data from these sites are scarce, especially for establishing the initial and boundary conditions.

In addition, it has been noted that, even if there were reliable simulation models that could predict the outcome of such disturbances, the input data requirements for such models would be formidable. For a realistic simulation of the conditions at Yucca Mountain under HTOM, it would be almost impossible to consider the number of fractures that need to be characterized with all their thermomechanical and hydrologic properties. Large changes in the stress field are imminent and the impact very uncertain. Further complications arise from the difficulty in establishing reliable initial chemical conditions.

The LTOM results in cooler waste package and rock temperatures; therefore, temperature effects on hydrologic, mechanical, and chemical processes can be predicted with greater certainty. However, using DOE's current waste canister spacing for the LTOM, the repository may need to be expanded to areas beyond those that have been characterized and identified with suitable host rocks. The cost of expanding the repository is expected to be formidable and the time delays lengthy.

This report summarizes preliminary work conducted in late 2001 and early 2002 for Nye County to evaluate the feasibility of alternative conceptual designs for a permanently-ventilated repository (PVR). Nye County's ultimate performance goals for a PVR design are to:

- Minimize the potential for human intrusion
- Provide stable underground openings
- Remove heat generated by the waste and keep the repository relatively cool.
- Minimize the area (footprint) and therefore the cost of the repository.

1.2 ORGANIZATION OF THE REPORT

This report is presented in seven main sections, which are followed by references and an appendix. Section 1.0 presents the introductory and background material related to the conceptualization of the PVR. Section 2.0 provides more detail on the PVR concepts and introduces various components of the system that need to be studied. Section 3.0 presents details of the major components introduced in Section 2.0. Section 3.0 leads into a description of the numerical model setup that is presented in Section 4.0. Section 4.0 also provides a description of the parameters needed for the PVR conceptual design analysis and presents some sources for these parameters. Section 5.0 presents the results of the simulations performed thus far in support of the PVR design. Section 6.0 summarizes the findings of this report. Section 7.0 presents recommendations for future work. Section 8.0 lists cited references. In Appendix A, a brief description of the theory and documentation of the atmospheric TOUGH2 (A-TOUGH2) code used for the analyses in this report is presented with supporting verification and validation runs.

2.0 PERMANENTLY-VENTILATED REPOSITORY DESIGN

The PVR conceptual design, discussed herein, only considers the geologic environment and the heat generated by the waste. This analysis does not address surface facilities, the waste emplacement process, and other important components and processes of the disposal system that are addressed by DOE (2001a). It is anticipated that these components and processes of the disposal system can be rather easily incorporated into the PVR design at a future date.

The PVR conceptual design discussed in this section assumes some baseline dimensions as a starting point. This design will be referred to as the baseline PVR design. The impacts of varying some of these dimensions will be discussed with supporting calculations in later sections of this report.

Figure 1 shows a schematic diagram of the proposed baseline PVR conceptual design overlaid on the current DOE baseline design for comparison and reference purposes. The PVR conceptual design provides a network of stable pathways for natural ventilation and minimizes direct contact of the ventilation air with the waste packages. In previous open repository designs (Montazer, 1996 and 1998), ventilation was applied through the waste package emplacement drifts throughout the main life of the repository (10,000 yr.). In the PVR design, an essentially separate network of tunnels, drifts, and shafts will be backfilled with highly porous and permeable rubble to provide ventilation during and after the pre-closure period. A majority of the drifts and shafts may be filled with rubble during the pre-closure period. Only access drifts and shafts will remain open during this period. After the pre-closure period, the entire network, except for the waste emplacement drifts, will be filled with rubble.

Direct ventilation of the emplacement boreholes or drifts will be applied only during the pre-closure period. The rubble backfill will provide rock mass stability without blocking air flow through the passages; it allows for natural ventilation. The rubble may consist of the broken tuff obtained during excavation of the tunnels, cobbles and boulders from Fortymile Wash, or other available and suitable rock material. Some components of the system, such as the intake drifts and exhaust shafts, may be constructed by rubble-producing mining techniques. These components are located far enough from the emplacement boreholes that their impact on the integrity of the repository host rock is not of concern.

The optimum size and number of the shafts, drifts, and tunnels have not yet been determined. These parameters will be estimated after more in-depth analytical and numerical modeling are performed. A preliminary assessment of the feasibility of the baseline PVR and some potential alternative designs are presented in this report. Further studies are needed to provide a comprehensive evaluation of an optimum PVR design.

The network of the rubble-filled openings consists of several intake drifts, tunnels, cross-drifts, and shafts. The portals for the intake drifts will be located in the various washes on the eastern slope of Yucca Mountain. It is preferred that the portals of these tunnels be on south-facing slopes.

The cross-drifts will provide the main cooling system for the waste packages. There will be no waste packages in any of these drifts. The number and spacing of the cross-drifts required

depends on the overall target temperature of the repository. A minimum safe distance of the drifts from the emplacement boreholes is assumed to be 10 m. Figure 2 shows schematic diagrams of two configurations of the preliminary spacing of the waste-emplacement boreholes and their positions relative to the ventilation drifts. The waste-emplacement boreholes will be approximately 2.5 m in diameter. This diameter is expected to be large enough to accommodate the waste package (about 1.5 m in diameter) and its associated protection system. However, the DOE (2001a) baseline design diameter of 5.5 m can also be used for the emplacement boreholes (or drifts) in the PVR design with only slight modifications.

In the PVR baseline design (Configuration A in Figure 2), there will be five emplacement boreholes between ventilation drifts. The ventilation drifts will, therefore, be approximately 70 m apart (from centerline to centerline). In the alternative PVR design (Configuration B in Figure 2), there will be two emplacement boreholes between ventilation drifts. In this case, the ventilation drifts will be approximately 30 m apart (from centerline to centerline). These dimensions are for testing purposes and other configurations may prove more optimal.

With these arrangements, and assuming that the total length of all the waste packages laid end to end is 60,000 m (DOE, 2001a), 60 waste-emplacement boreholes—each 1,000 m long—will be needed to store the waste. The waste-emplacement boreholes need not have a continuous length of 1,000 m; rather, they can be drilled at lengths of 500 m or less (depending on feasibility) from the north-south drifts. Four of these north-south drifts are shown in Figure 1.

Figure 3 shows the conceptual arrangements of the waste-emplacement boreholes and ventilation drifts for baseline Configuration A and alternative Configuration B. In the Configuration A conceptual design, the width of the waste-emplacement area is 840 m—less than 1 km. The total emplacement area is approximately 208 acres.

Similarly, for Configuration B, the width of the waste emplacement area is 900 m. The total emplacement area is approximately 222 acres.

These emplacement areas are estimated without considering the need for a buffer zone around the repository. Also, some areas within the proposed host rock are not suitable for waste emplacement and may need to be avoided. Assuming about 10% of the footprint will be used to satisfy these needs, the total area requirement for these cases is less than 250 acres. With these assumptions, the area required for these two configurations is approximately one-fifth the size of the smallest area estimated in DOE (2001a) for HTOM (1,150 acres) and approximately one-tenth of that estimated for LTOM (2,500 acres).

In both configurations, heat-load can be reduced by increasing the longitudinal spacing of the canisters. Increasing the canister spacing will increase the repository footprint area. It is assumed that the heat load is reduced proportionally to the inverse of the canister spacing. That is, if the spacing of the canisters is doubled, the heat load is reduced by 50%. The waste emplacement area is also assumed to increase proportionally to the inverse of the heat load. That is, if the heat load is to be reduced by 50%, the emplacement area should be doubled. Obviously, the number and/or lengths of the ventilation drifts and waste emplacement boreholes will increase proportionally. These assumptions are made to facilitate the comparison of various configurations and heat loading scenarios presented in this report. In the actual disposal

scenario, the geometric shape of the repository footprint area, which may not necessarily be rectangular, will change these ratios.

The baseline PVR design is presented as a starting point for analysis. Details of various components of the proposed PVR will be discussed in the following sections. It should be emphasized that this is a preliminary conceptual design that will be refined as performance analyses are completed.

3.0 MAJOR COMPONENTS OF THE PERMANENTLY-VENTILATED REPOSITORY DESIGN

In this section, major components of the PVR conceptual design are briefly reviewed. These components are illustrated in Figures 1 and 4 and include:

- Intake drifts
- Waste-emplacement drifts or boreholes
- Ventilation cross drifts (both open and rubble-filled)
- Exhaust drifts, shafts, and chimneys
- Drainage system.

These components are described independently of specific PVR configurations in the following sections.

3.1 INTAKE DRIFTS

In the conceptual design, the intake drifts are nearly horizontal large-diameter drifts that will supply outside air into the repository. Currently, they are considered to be approximately 8.5 m (25 ft) in diameter. The reason for selecting this diameter is the success of the Exploratory Studies Facility with a tunnel-boring machine of this size. However, the drifts can be larger and need not be excavated with a tunnel-boring machine. Because their purpose is merely to supply air into the repository area, they can be excavated by conventional mining techniques that are designed to produce rubble zones in the host rock. These drifts must slope slightly downward in order to reach the repository horizon from higher elevation portals on the east flank of Yucca Mountain. However, the drifts should slope upward toward the repository after passing through the Paintbrush Tuff nonwelded (PTn) unit (Figure 4). The reason for this is to avoid redirecting any moisture that may be intercepted by the drifts into the repository area as a result of potential lateral moisture flow in the PTn unit. A north-south drainage drift may be required to collect any seepage from this unit and direct it away from the repository (Figure 4). At the south end of the drainage drift, an infiltration gallery should be installed to percolate any potential water from the PTn unit down to deeper formations. The area required by the infiltration gallery depends on the magnitude of the potential lateral moisture flow along the PTn unit.

The following parameters must be established prior to designing the drifts:

- The amount of air flow required to maintain the repository at a specific temperature
- The air permeability of the rubble-filled drifts
- The size and number of drifts required
- The size of rubble to be used to fill the openings
- The size and location of the underground infiltration/percolation gallery
- The infiltration capacity of the gallery.

These parameters will be addressed in future reports.

3.2 EMPLACEMENT BOREHOLES

The emplacement boreholes used in the baseline design are depicted conceptually in Figures 5 and 6. Figure 5 shows a simplified arrangement of the waste-emplacement boreholes and their relation to the rubble-filled drifts. Figure 6 shows various components of a typical waste-emplacement borehole. In the conceptual design, the borehole is approximately 2.5 m in diameter and is about 500 m long. This borehole will be cased. The material to be used for this casing should be highly resistant to corrosion. The wall of the casing should be at least 1.3 cm (0.5 in.) thick; the actual thickness will depend on the strength of the material to be used. The casing should be designed to allow for thermal expansion and to withstand the rock stresses that tend to close the borehole.

The current concept is that the waste-emplacement boreholes will be cased. The waste packages are inserted into the casing via a roller/skid system. This system will be designed to centralize the canisters. The specifics of this emplacement system are not addressed in this report.

It is expected that the emplacement boreholes will be ventilated during the pre-closure period of the repository. After the pre-closure monitoring period, the cased boreholes will be capped with secure, gas-tight caps. The purpose of this cap is to minimize the potential escape of gaseous radionuclides into the ventilation system. A secure check valve will be installed in the cap to enable purging and pressurizing the casing with a dry inert gas. Nitrogen or another inert gas may be used to purge and pressurize the system. The purpose of the pressurization is to delay and minimize the entry of moist air from the moist rock into the casing during the initial stage of storage before significant heating and drying of the rock occurs. The type of gas chosen must not produce radioactive isotopes as a result of radiation potentially emitted from the radioactive waste. For example, nitrogen may not be suitable because it could produce carbon-14 if exposed to radiation.

The end caps may be equipped with fanned-heat sinks (Figure 5) that will be exposed to the ventilation air stream. Large-diameter copper rods may be used in the emplacement boreholes to promote heat transfer to the end caps. However, the interaction of the copper with the waste package may not be desirable. The suitability of material in the waste-emplacement boreholes will not be further addressed in the baseline PVR conceptual design. However, the potential heat transfer along such material will need to be estimated and its advantages and disadvantages evaluated.

Immediately following the drilling and/or mining of waste-emplacement boreholes or drifts, the matric potential and saturation in the formation walls will be relatively high and the humidity of the air is expected to be near 100%. Prior to installing the casing in the waste-emplacement boreholes or lining of the emplacement drifts, the boreholes should be ventilated for a period of time to dry out the host rock sufficiently. Once a relatively dry skin is developed around the boreholes (about 0.5 m), the ambient air in these openings will have a low relative humidity, provided ventilation continues. After installation of casing, the more humid air from the host rock beyond the dried-out skin will tend to move toward the opening. However, after emplacement of the waste, the heat generated by the waste will move this more humid air away from the emplacement openings toward the air stream in the naturally-ventilated drifts.

Therefore, proximity to a ventilated drift is important for removal of the humid air and heat. This process will continue to dry out the rock in the vicinity of the waste-emplacement openings.

The diameter of the waste-emplacement boreholes was selected to reduce the cost of excavation and to increase the stability of the waste-emplacement opening. Additional analyses beyond the scope of this study will be required to optimize the borehole diameters as well as to evaluate the following parameters:

- The length of time required to dry the rock mass near the boreholes prior to waste emplacement
- The optimum spacing of the boreholes
- The spacing required if larger-diameter openings will be used
- The range of temperatures to be expected at the wall of the openings
- Specification of the casing material
- Diameter and length of copper rods
- Thickness of the casing wall
- Mechanics of the skid/roller system.

3.3 VENTILATION NORTH-SOUTH AND CROSS DRIFTS

The purpose of the ventilation drifts, including major north-south drifts and east-west cross drifts illustrated in Figure 1, is to direct the relatively cool and dry air that is supplied by the intake drifts to the waste-emplacement area of the repository. The east-west cross drifts will serve to remove heat and moisture from the repository horizon. The north-south drifts will serve as access for drilling the waste-emplacement boreholes, waste emplacement operation, and enhancing the air flow between the east-west cross drifts. These north-south drifts should be constructed more carefully because they need to stay open and operational during the pre-closure period. These drifts may be lined with steel sets that are connected horizontally by steel bars. The purpose of this lining is to increase the thermal conductivity of these drifts and promote heat transfer from the rock to the air stream. It may be possible to use copper, if it is proved durable and environmentally safe in these drifts. It is expected that the heat conduction along such a metallic lining would substantially increase the heat dissipation. The effectiveness of the heat conductors will need to be evaluated with the ventilation model in the future.

Ventilation drift-related parameters that should be evaluated in future studies include:

- The number of ventilation drifts
- The optimum size of the drifts
- The impact of the intermediate horizontal ventilation drifts above the repository horizon
- Effectiveness of the heat sinks
- Thickness and extent of the heat-sink lining.

3.4 EXHAUST SHAFTS

The purpose of the exhaust shafts is to direct the warm and moist air to the outside atmosphere. The larger the difference in elevation between the exhaust and intake points, the more efficient the ventilation system will be. In the baseline PVR design, the exhaust shafts are designed to minimize disturbance of the PTn unit. The PTn unit is believed to provide protection against large groundwater infiltration events; its integrity should be maintained as much as possible. For this reason, the exhaust shafts are designed to exit Yucca Mountain through the Topopah Spring welded (TSw) unit that underlies the PTn unit (Figure 4). The exhaust shafts will be connected to the ventilation drifts at two levels (Figure 7) to minimize direct vertical connection to the underground area (as proposed by Montazer, 1998).

A portion of the ventilation exhaust system will need to slope upward to increase the elevation difference (Figures 8 and 9). At approximately the final 50 m (150 ft), the exhaust system should slope downward to minimize the entry of surface water. The exhaust shafts may be connected to a series of chimneys constructed along the western slope of Yucca Mountain. These chimneys should be constructed in the rock and covered by reinforced concrete and talus to prevent erosion and to increase stability (Figure 9). Talus and rubble will cover the final exit of these chimneys to minimize the potential for human intrusion and exposure to environmental elements.

Exhaust shaft-related parameters that should be evaluated in future studies include:

- The number of exhaust drifts
- The optimum size of the shafts
- The minimum elevation difference required between the air entry and the exhaust points
- The impact of the intermediate horizontal ventilation drifts above the repository horizon
- Thickness and extent of the heat-sink lining.

3.5 DRAINAGE SYSTEM

A drainage system is optional. At a minimum, a drainage system may divert potential seepage from the PTn unit away from the ventilation drifts, as discussed above and shown in Figure 4. In this case, the drainage system does not need to be connected to the land surface, because the amount of flow is expected to be minimal and can be diverted into an underground infiltration gallery.

In addition, an expanded drainage system may also be required to minimize potential disruption of the ventilation system in case of a water table rise to the repository horizon. Although such a rise is considered very unlikely based on the current understanding of Yucca Mountain hydrology, the emplacement of a drainage system will ensure that the water table will never rise to the repository level. In this case, the expanded drainage system must be connected to the land surface because the quantity of water potentially could be large.

Finally, the expanded drainage system may also help in diverting a low-viscosity, small-volume volcanic intrusion away from the repository. Low viscosity intrusions tend to behave as a viscous liquid. If the permeability of the drainage system is adequate, a relatively large amount

of lava may be diverted away from the repository area and out to a low-lying area east of Yucca Mountain.

The main disadvantage of the expanded drainage system is that it provides a direct pathway to the accessible environment. Sloping the portion that underlies the repository away from the repository can minimize this disadvantage. However, the benefits may not justify the risks. Since the rise of the water table is considered very unlikely, an extensive drainage system is considered optional and is included only in the interest of completeness. It will not be considered further in this report.

3.6 ADDITIONAL ISSUES TO BE CONSIDERED

The following issues are not addressed in this report but should be considered in future PVR studies.

3.6.1 Potential for Gaseous Radionuclide Migration

In any form of a ventilated repository, gaseous radionuclide migration is of concern. The plan is for the naturally-ventilated repository to operate at temperatures such that iodine should not be of concern; however, rigorous analysis will be required to address the potential risk of iodine. The generation of radon gas also may be a concern and should be evaluated. It is possible that the amount of radon in the host rock is significantly larger than that potentially produced by the radioactive waste. However, these potential risks should be evaluated for future designs.

3.6.2 Maintenance of Rubble Permeability

Although the rubble can be designed to attain very high air permeability, the persistence of high air permeability for a long period needs to be evaluated. In future work, the grain-size distribution of the rubble will be studied and an optimum range of size distribution determined, based on empirical calculations. However, the efficiency of the rubble-filled cross drifts and major north-south ventilation drifts is expected to decline with time. Future tests and analyses will be required to address long-term efficiency of the ventilation system.

The growth of plants and microorganisms near the entrances of the intake drifts, exhaust shafts, and chimneys is of concern. In nature, such growth has not been observed over the talus slopes of Yucca Mountain; however, the potential for plugging of the ventilation system with microorganisms and plant growth near the entrance needs to be evaluated.

Along the eastern flank of Yucca Mountain, the Tiva Canyon welded (TCw) unit is the most likely candidate for the entry portals. This unit is highly fractured, especially near the surface, and plugging of the entry portals to the ventilation system will probably not be of concern. This assumption will be evaluated in the future by using the air permeability and infiltration data that have been obtained by various DOE investigators.

Volcanic intrusions can severely damage the efficiency of the ventilation system. For this reason, the drainage system discussed above may be essential if the potential for volcanic intrusions is considered relevant. The drainage system can intercept small volume intrusions

only once. The efficiency of the drainage system will be reduced significantly, if it is flooded with lava.

3.6.3 Talus Slopes

The entry and exit slopes will need to be constructed with steep angles of repose to minimize vegetation growth. In addition, it is recommended that the rocks used to cover these slopes be of the dark desert varnish-covered type to increase solar absorption. The heat during the day will help dry the intake air. On the other hand, this will also increase the temperature of the intake air slightly. These design parameters and concerns should be evaluated in the future.

4.0 NUMERICAL MODEL MESH AND PARAMETERS

In this section, the preliminary model, including mesh, nodes, and boundaries that encompass some of the components outlined in the previous sections, will be presented. In addition, the design parameters needed to support the baseline and other PVR conceptual design configurations and to serve as input parameters for the numerical model are described. The data from which design parameters have been selected are identified. Ranges in baseline design parameters are also described.

4.1 MODEL MESH AND DESCRIPTION OF MESH SETUP

Figure 8 shows the outline of the overall model domain of interest overlaid on a simplified geologic cross section of Yucca Mountain. The baseline model domain is approximately 3,000 m wide in the east-west direction and 2,000 m in the north-south direction. Figure 10 shows the plan view of the model domain of interest overlaid on a simplified geologic map of the site. The boundary of the repository is purposely set larger than either one of the configurations presented in Figure 3 to allow for testing more expanded alternatives if needed.

In this report, the feasibility of the baseline and other PVR configurations is evaluated by numerical modeling of only portions of the total domain. A full-scale model of the entire domain of interest is planned for the near future.

Four basic mesh setups were used for various purposes. Two of the mesh configurations were set up in both two and three dimensions. Only the results of one successful two-dimensional mesh (Mesh 4) will be presented in this report. For traceability and quality assurance purposes, the numbers of the meshes are retained in this report.

4.1.1 Description of Mesh 4

Mesh 4 (Figure 11) is referred to as the refined north-south mesh; it consists of 40 columns 10-m wide and 24 rows 22.5-m high. Figure 11 also shows the location of the elements designated as the ventilation drifts and the waste-emplacement boreholes. The arrangement shown in this figure corresponds to Configuration A of the baseline PVR design. These elements were turned on or off depending on their desired representation. When the ventilation elements were turned off, they were replaced by the host-rock (TSw) properties. When used to simulate a ventilation drift, they were replaced by an element with atmospheric properties (see Appendix A). The spacing between the ventilation drift elements is 70 m in this configuration.

The waste-emplacement elements (they will be referred to as heaters in the following sections) have the properties of host rock. Various waste-emplacement and heat-loading scenarios were simulated by applying a temporally variable heat source to the center of these elements and varying the strength of the heat source.

The mesh for Configuration B of the PVR design (Figure 2) differs only in its number of ventilation drifts and waste-emplacement nodes and is not shown in Figure 11. For Configuration B, the number of the elements representing ventilation drifts was increased to 11 and their spacing reduced to 30 m.

4.1.2 Boundary Conditions

The physical boundaries are set as shown in Figure 11. The lateral edges are both adiabatic for heat transfer and "no flow" for hydrologic boundaries. The upper edge of the domain is modeled as the top of the PTn unit. The lower model boundary is the uppermost layer of the Calico Hills nonwelded (CHnw) unit. The upper and lower boundaries have constant conditions with time, as defined in Table 1. At the upper boundary, a percolation flux is applied directly to the PTn unit. Percolation rates of 4.6 mm/yr. (mean) and 10.1 mm/yr. (upper bound) (DOE, 2000a) were used. However, for the preliminary analyses of the heat loading, only the upper bound percolation rate (10.1 mm/yr.) was used. Sensitivity analyses will be performed in the near future.

4.1.3 Initial Conditions

The initial conditions were set up using a simplified mesh similar to Mesh 4, but with much wider mesh elements. Only matrix properties were used for this case. By applying the upper bound infiltration flux to the PTn layer, the simulation was run until near steady-state conditions were achieved for temperature, pressure, and saturation. As will be discussed below, these steady-state conditions were used as initial conditions in subsequent calculations. To achieve steady-state initial conditions, no ventilation drifts were used; the properties of the elements identified as ventilation were set to represent the TSw unit during initialization simulations.

4.2 PARAMETERS AND DATA

This section summarizes the data and references used for the baseline study. These data were obtained both from DOE (2001b), and from Yucca Mountain databases and reports. Simplifications were made and averages were taken of some of the material properties to facilitate the computations.

4.2.1 Unsaturated Zone Rock Properties

The unsaturated zone data are available from the Yucca Mountain unsaturated zone site scale model (DOE, 2000a). Table 2 summarizes the hydraulic parameters for the matrix of the hydrogeologic units of concern. Table 3 provides the fracture properties for these hydrogeologic units.

The standard deviation of the logarithm of the measured permeability values of the TSw unit ranges from 0.9 to 3.6 for matrix, and 0.3 to 0.7 for fractures within the unit (DOE, 2000b). These ranges in the permeability will be used in future sensitivity analyses. Thermal properties of the hydrogeologic units are listed in Table 4. Only the mean values are used for the simulations presented in this report.

4.2.2 Waste Emplacement Boreholes

Emplacement boreholes were simulated by applying a heat load to the corresponding elements in the model. Different heat-load histories were considered. The heat-load histories used for each simulation are presented and discussed in Section 5.0.

For a number of simulations, the heat load was applied to emplacement boreholes only after a pre-closure period. During this pre-closure period, it was assumed that the emplacement boreholes were directly ventilated and all heat generated by the waste was removed by this ventilation. The assumption that direct ventilation of emplacement boreholes would remove all heat was based on the analyses made by NWRPO (1998). After this pre-closure period, it is assumed that waste emplacement boreholes are sealed and not ventilated; only ventilation cross-drifts are ventilated.

4.2.3 Ventilation-Related Parameters

Ventilation was applied by using the atmospheric simulation capabilities of A-TOUGH2 (see Appendix A). In this case, the model calculated the ventilation flow rates, which were controlled by the pressure and temperature gradients between the simulated drift and the host-rock elements. In the ventilation drifts, an eddy diffusivity of 0.01 cm^2/s was used to calculate both the heat and mass transfer coefficients. All ventilation drifts, intake shafts, and exhaust shafts were assumed to be filled with the same type of rubble. For flow through the rubble, it was assumed that applying this eddy diffusivity was a reasonable simplification. It should be noted that eddy diffusivity is dependent on velocity of the moving air and the temperature and pressure gradients. These dependencies were not considered for this study and should be evaluated in future work.

4.2.3.1 Rubble Backfill

Table 5 lists some of the properties, including rubble properties, used by DOE (2000c) for the engineered barrier system. The properties used in simulations described in this report are noted in Table 5. Moisture characteristic data for rubble are very scarce; therefore, for the simulations presented in this report, it was assumed that there is no liquid flow through the rubble. The air permeability of the rubble was set to 1.0×10^{-5} m^2.

4.2.3.2 Intake Drifts

The intake drifts were not simulated in the baseline analyses presented in this report. It was assumed that the ventilation air entering the repository area had a constant temperature of 18.7°C and a humidity of 0.30%. Future calculations are needed to justify these assumptions.

4.2.3.3 Exhaust Drifts, Shafts, and Chimneys

The simulation of exhaust drifts, shafts, and chimneys were not developed in this baseline study. Future studies will incorporate these features.

4.2.3.4 Ventilation Drifts

In the conceptual PVR configurations, the diameter of the ventilation drifts was set to 8.5 m. In simulations presented in this report, these drifts were represented by an array of rectangular elements 10 m in width, with a constant height of 22.5 m. The area of this rectangle (225 m^2) is equivalent to the area of four 8.5-m diameter drifts. The perimeter of this rectangle (65 m) is equivalent to the perimeter of 2.5 drifts with 8.5-m diameter. Because of the two-dimensional

nature of the simulations, the perimeter has more influence on the outcome. The effect of these approximations, which are the result of simplification of the mesh, are not expected to be significant. This will be investigated in future work.

4.2.3.5 Drainage System

The drainage system was not simulated for this study and needs to be considered in future studies, as outlined in Section 3.0.

4.2.3.6 Waste Package Heat Load

The heat load was assumed to be removed by ventilation during the pre-closure period. Upon closure, the heat load applied per meter length of drift over time is shown in Table 6. For example, after 100 yr. of pre-closure, the heat load applied is approximately 379 W/m, or nearly a five-fold reduction, assuming 0 yr. of pre-closure.

The values in Table 6 are considered to be the full heat load. Many of the simulations considered application of only a portion of the full heat load. Longitudinal proportioning of the heat load was accomplished by dividing all the values in Table 6 by a constant factor. Between each time step, the power was linearly interpolated. A-TOUGH2 provides an option to fit a spline curve to the transient boundary conditions. This capability was only used for the atmospheric elements.

In DOE (2001a), a phased disposal was considered. In these plans, there is a lag time between when the waste arrives at the site and when it is emplaced in the underground facility. During this time period, the waste is temporarily stored in an aboveground facility. This time-phased disposal was not considered in the simulations presented in this report. Natural ventilation during this aboveground disposal time period could be used to cool and dry the emplacement borehole/drifts before they are used for disposal.

4.2.3.7 Additional Assumptions

For the purpose of this analysis, it is assumed that 97,000 metric tons of uranium (MTU) inventory can be placed in 60 or more emplacement boreholes/drifts.

5.0 SIMULATION RESULTS

More than 100 simulations were made for this study. Most of these simulations were experimental setups of various parameters. Both the upper-limit infiltration rate and mean permeability values were used for these experimental cases. After setting up quasi-steady-state initial conditions, simple calculations were used to estimate the spacing of the drifts/boreholes by applying various heat loading scenarios. However, for the heat loading and ventilation drift spacing calculations, only the upper limit infiltration and mean permeability were used.

Table 7 summarizes the pertinent simulations that were useful for evaluation of the initialization of the problem and for estimation of the drift spacing and the impact of varying heat load. This table includes simulation file number, simulation number, and figure numbers for cases that are presented in this section. The simulation file number is included only for traceability, future reference, and quality assurance purposes.

Major performance objectives of a successful PVR design (Section 1.0) include providing a low-temperature repository that has a substantially smaller footprint than those presented by DOE in the science and engineering report of 2001 (DOE, 2001a). It should be emphasized that the preliminary results presented here do not provide conclusive estimates of the magnitude of the operating temperature and the footprint area of the repository. However, they provide an indication of the feasibility of the concept of the PVR in lowering the operating temperature of the repository and reducing its footprint size. Most of these simulations ran for relatively short periods. Once the optimum configuration is selected, it will be run for at least 10,000 yr.

Various sensitivity analyses were performed using the coarse mesh. For example, the effect of turning off eddy diffusivity significantly reduced the efficiency of heat removal from the rock. The results of these analyses are not presented in this report.

5.1 EFFECT OF THERMAL LOADING USING MESH 4

Mesh 4 was designed to represent the relative distribution of the waste-emplacement boreholes and the ventilation drifts, as prescribed in the original baseline PVR design. Various simulations were made changing the heat loading of the waste-emplacement boreholes. In the first group of simulations discussed below, the arrangement of the emplacement boreholes and the ventilation drifts are close to the original baseline PVR design.

In Simulation Number 8 (Table 7), a 50-yr. period of pre-closure was considered. In this simulation, six waste-emplacement boreholes were used between the ventilation drifts instead of the original five prescribed for the baseline PVR design.

The heat loading history used for Simulation Number 8 is shown in Figure 12, which is equivalent to 25% of the full heat load. Because six waste-emplacement boreholes were used for this case, the heat load is equivalent to 30% of the baseline PVR (6/5 of 25%). This means that, for this case, 3.33 times the footprint area of the original baseline PVR (or 833 acres) is required for the repository. The heating actually began at approximately 40 yr. after emplacement and gradually increased to 25% of the predicted values at 50 yr. (Table 6) to facilitate modeling a rapid temperature change.

Figure 13 shows the temperature distribution and Figure 14 shows profiles of temperature through a ventilation drift element and through a waste-emplacement borehole element. The temperature variations are shown for the first 62.5 yr. (12.5 yr. after pre-closure). These figures show that temperature rises to near 100°C over a short period of time (approximately 12.5 yr. after closure). Profile 2 in Figure 14 intersects the heater closest to the ventilation drift and, therefore, shows relatively cooler temperatures than Profile 3, which is located approximately midway between ventilation drifts. Because the simulated temperature approached boiling and did not provide a significant savings in the area of the repository, it was decided that the spacing of the waste-emplacement boreholes and the ventilation drifts of the baseline PVR was unacceptable.

Figure 15 shows vertical profiles of saturation through a drift and a waste-emplacement borehole for this simulation. The length of simulation time is too short to see any impact on the saturation changes.

Two additional simulations were made using pre-closure periods of 150 and 300 yr. As mentioned previously, during the pre-closure period the heat loading was assumed negligible, because ventilation of the emplacement boreholes is assumed to remove the heat generated by the waste.

Figure 16 shows the heat loading for a case in which heat loading was assumed negligible during the 150-yr. pre-closure period (Simulation Number 9, Table 7). Figure 17 shows the distribution of temperature for this case. Temperature in the vicinity of the waste-emplacement boreholes approaches 82°C after 420 yr. (270 yr. after closure of the repository). Profiles of temperature and saturation are shown in Figures 18 and 19, respectively. Again, Profile 2 shows cooler temperatures than Profile 3 because Profile 2 is closer to a ventilation drift. These temperatures are more reasonable than previous cases and are slightly below the LTOM design (85°C). The acreage requirement (833 acres) is about one-third of the DOE LTOM design (2,500 acres).

Figure 20 shows the heat loading history for another case in which heat loading was assumed negligible during the 300-yr. pre-closure period (Simulation Number 10, Table 7). It should be noted that the ramp-up of heat beginning at 250 yr. is to smooth-out the simulation process and is not intended to represent actual predicted heat loading. The results for this case are shown in Figure 21. The temperature remains below 30°C for the first 727 yr. Although simulation times were not extended beyond this time, temperatures are not expected to rise above 30°C after this period. The area requirement for this case is still 833 acres.

5.2 ALTERNATIVE SPACING WITH MESH 4

Mesh 4 was slightly modified to evaluate the effect of alternative spacing between the ventilation drifts and the waste-emplacement boreholes. Two separate heat-loading scenarios were used. The first scenario (Simulation Number 13, Table 7) used fully loaded waste-emplacement boreholes with a 250-yr. pre-closure period. The second case (Simulation Number 14, Table 7) used 50% linear loading (Figure 22).

The mesh and the results of Simulation Number 14 are shown in Figures 23 and 24. As shown on the left-hand side of Figure 23, there are only two waste-emplacement boreholes placed

between every pair of ventilation drift elements. The spacing between the drifts is reduced to 30 m in this case. It is estimated that for full loading in this arrangement, the area requirement is 250 acres (which is the original area of the baseline PVR) but the temperature rises to above 90°C (Table 7).

With 50% heat loading, the temperature remains near 55°C for the first 720 yr. (and is not expected to increase significantly over a longer time interval), but the acreage requirement is estimated to be about 500 acres. This area is twice the original baseline PVR, but is still 20% of the DOE LTOM and less than 44% of the DOE HTOM. This seems to be a reasonable scenario; however, the assumptions used for these calculations require rigorous evaluation and verification.

6.0 DISCUSSION OF RESULTS

In general, it was found that, with the assumptions used for the simulations in this report, it is not easy to remove heat from emplacement boreholes by predominantly conductive heat flow. This finding is consistent with the low thermal conductivity of the TSw unit (about 2 W/m K). This low thermal conductivity causes heat to accumulate over a relatively short period near the emplacement boreholes. With 10-m minimum distance to the nearest ventilation drift (maintained at 20°C), the heat load to maintain the repository host rock below boiling temperatures is estimated to be around 200 W/m of emplacement borehole. A fully-loaded emplacement borehole (i.e., placement of the canisters end to end, with no spacing) produces a heat load of 1,500 W/m initially. The heat load drops down to below 400 W/m after about 100 yr. For this reason, during the initial 100 yr., the heat production is much larger than what the thermal conductivity of the host rocks allows to be transmitted away. To increase the heat transfer, the distance to the ventilation drift needs to be decreased significantly to about 2 to 3 m; however, drifts this close are not considered safe for operational purposes.

One alternative is to load the emplacement boreholes with only about 10% of the heat load, which increases the footprint of the repository to about 10 times that conceived in the baseline PVR design (from 250 to 2,500 acres). This is what DOE has predicted for the LTOM case, which is not acceptable to Nye County.

Another alternative is to modify the proposed conceptual design of the PVR to allow for indefinite ventilation of the emplacement boreholes. Although this would be similar to Nye County's original design (NWRPO, 1998), the closure of the repository could be achieved by partially filling the drifts with rubble. It is believed that the rubble-filled drifts can provide both long-term mechanical stability as well as adequate long-term ventilation to achieve a permanently ventilated and closed repository.

Finally, in this report, preliminary simulations demonstrated that reasonably low temperatures and significant reduction in the acreage requirements might be achieved by the PVR design. This may be accomplished by increasing the number of rubble-filled ventilation drifts, reducing the number of waste-emplacement boreholes in between these drifts, and extending the pre-closure direct ventilation of the waste-emplacement boreholes. For example, preliminary analyses indicated that with 250-yr. pre-closure ventilation and using a footprint of about 500 acres, natural ventilation might sustain the temperature of the host rock below 55°C. For this case, 31 rubble-filled ventilation drifts (each with an area equivalent to four times that of an 8.5-m diameter drift), and 60 emplacement boreholes (each 2,000 m long) are required.

7.0 RECOMMENDATIONS FOR FUTURE STUDIES

It is recommended that the original Nye County ventilation simulation (NWRPO, 1998) be combined with the modified PVR design to provide removal of the heat from the waste-emplacement drifts. In the original Nye County ventilation simulation, the emplacement drifts were 8.5 m in diameter. A smaller diameter (e.g., 5.5 m) may be used for comparison purposes. For simulation purposes, the drifts need to be discretized. This discretization is necessary to properly calculate the interaction of the waste canisters with the host rock. The PVR rubble-filled drifts can be used to remove long-term heat generated by the waste and to maintain a relatively dry environment for the canisters. The only change in the overall design of the mesh would be the addition of ventilation to the waste-emplacement drifts.

The initial conditions achieved by using the simplified rock properties and the simulations developed for this project should be used to develop the three-dimensional model, which is needed to evaluate the modified PVR design. Further evaluation needs to be performed to determine the importance of various parameters, including eddy diffusivity, rubble properties, and optimum placement of the intake drifts, exhaust shafts, and chimneys.

The role of fractures in heat and moisture transfer have not been fully evaluated. It is possible that by incorporating the fractures into the model, the convective heat transport may reduce the temperature significantly. In addition, the following tasks should be considered in future work:

- Sensitivity analyses to evaluate the effect of varying the thermal properties of the hydrogeologic units
- Sensitivity analyses to assess the impact of varying percolation rates
- Evaluation of the velocity dependency of eddy diffusivity on simulation results
- Modification of A-TOUGH2 splining capability to smooth out the heat loading process and to minimize convergence problems
- Evaluation of the use of actual observed mean pressure, temperature, and humidity of the Yucca Mountain atmosphere and its long-term impact on the efficiency of the ventilation system
- Sensitivity analyses to evaluate the effects of varying rubble properties
- Evaluation of the effectiveness of the intake drifts, exhaust shafts, chimneys, and north-south drifts in the three-dimensional simulations
- Investigation of the effect of the actual size of the drifts on simulation results
- Calculation of the size and nature of the basic drainage system needed, as well as the capacity of the infiltration gallery required
- Evaluation of effect of time-phased waste emplacement on application of heat load.

8.0 REFERENCES

10 CFR (Code of Federal Regulations) Part 63.111 (e)(1). Washington, D.C.: U.S. Government Printing Office.

DOE (U.S. Department of Energy). 2000a. *Unsaturated Zone Flow and Transport Model Process Model Report*. TDR-NBS-HS-000002 Rev 00 ICN 02. Las Vegas, Nevada: U.S. Department of Energy, Yucca Mountain Project. Accessed November 2, 2001. http://www.ymp.gov/reference/index.htm.

DOE. 2000b. *Calibrated Properties Model Analysis and Model Report*. DOE/MDL-NBS-HS-000003 REV 00. Las Vegas, Nevada: U.S. Department of Energy, Yucca Mountain Project.

DOE. 2000c. *Overall Subsurface Ventilation System.* ANL-SVS-HV-00002 REV 00/01. Las Vegas, Nevada: U.S. Department of Energy, Yucca Mountain Project. Accessed November 2, 2001. http://www.ymp.gov/reference/index.htm.

DOE. 2001a. *Yucca Mountain Science and Engineering Report, Technical Information Supporting Site Recommendation Consideration.* DOE/RW-0539. Office of Civilian Radioactive Waste Management, Las Vegas, Nevada: U.S. Department of Energy, Yucca Mountain Project.

DOE. 2001b. *Automated Technical Data Tracking System (ATDT) Technical Data Information*. Las Vegas, Nevada: Yucca Mountain Project. Accessed November 2, 2001. http://www.ymp.gov/reference/index.htm.

Montazer, P. 1996. *Method and Apparatus for Generating Electrical Energy from Nuclear Waste while Enhancing Safety*, U.S. Patent office, Application Number 769868.

Montazer, P. 1998. *Method and Apparatus for Generating Electrical Energy from Nuclear Waste while Enhancing Safety*, U.S. Patent office, Patent Number 5,771,265.

NRC (Nuclear Regulatory Commission). 2001. 66 Federal Register 55743. Published on Friday 11/02/01.

NWRPO (Nye County Nuclear Waste Repository Project Office). 1996. *Annual Report of the Nye County Nuclear Waste Repository Project Office Independent Scientific Investigations Program.* Pahrump, Nevada: Nye County Department of Natural Resources.

NWRPO. 1998. *Annual Report, May 1997–April 1998, Nye County Nuclear Waste Repository Project Office Independent Scientific Investigations Program.* Pahrump, Nevada: Nye County Department of Natural Resources.

INTENTIONALLY LEFT BLANK

FIGURES

INTENTIONALLY LEFT BLANK

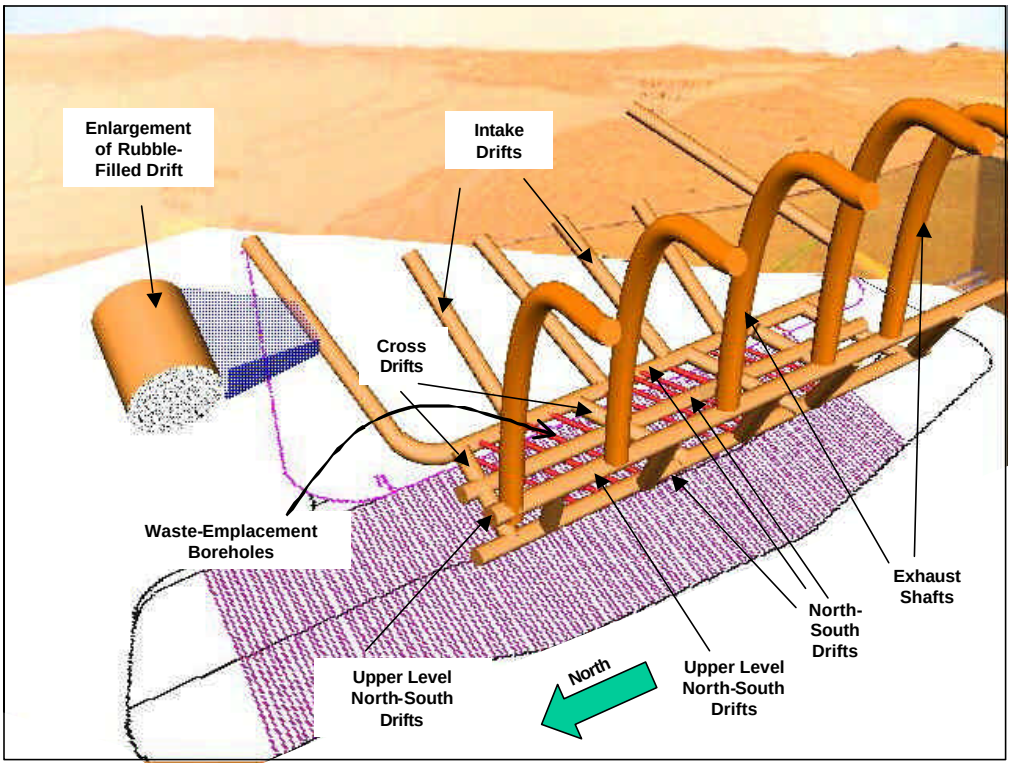

Figure 1
Schematic Diagram of the Conceptual Naturally-Ventilated Repository Overlying the Baseline U.S. Department of Energy Design

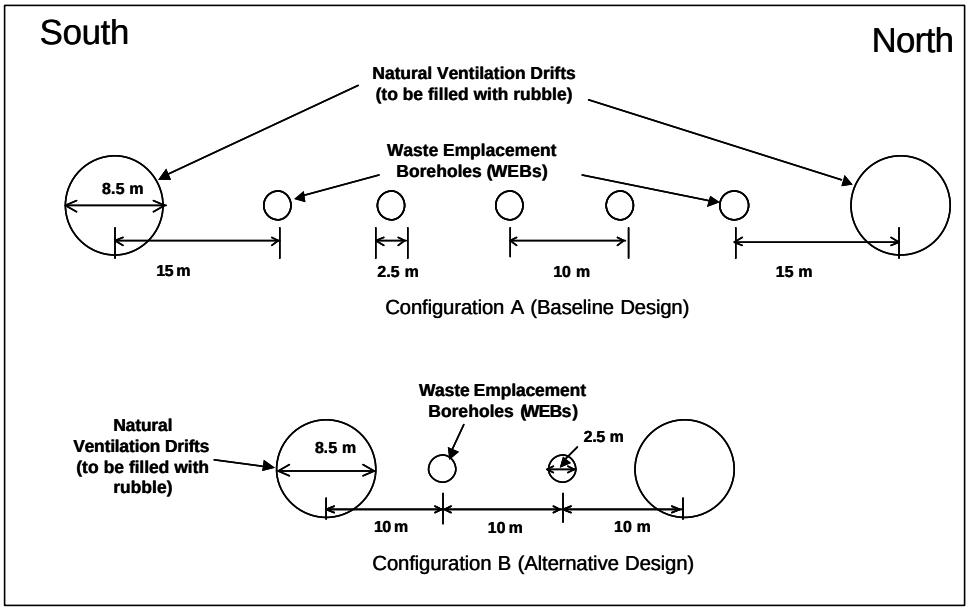

Figure 2
Schematic Cross Sections of Two Configurations Considered for the Conceptual Naturally-Ventilated Repository

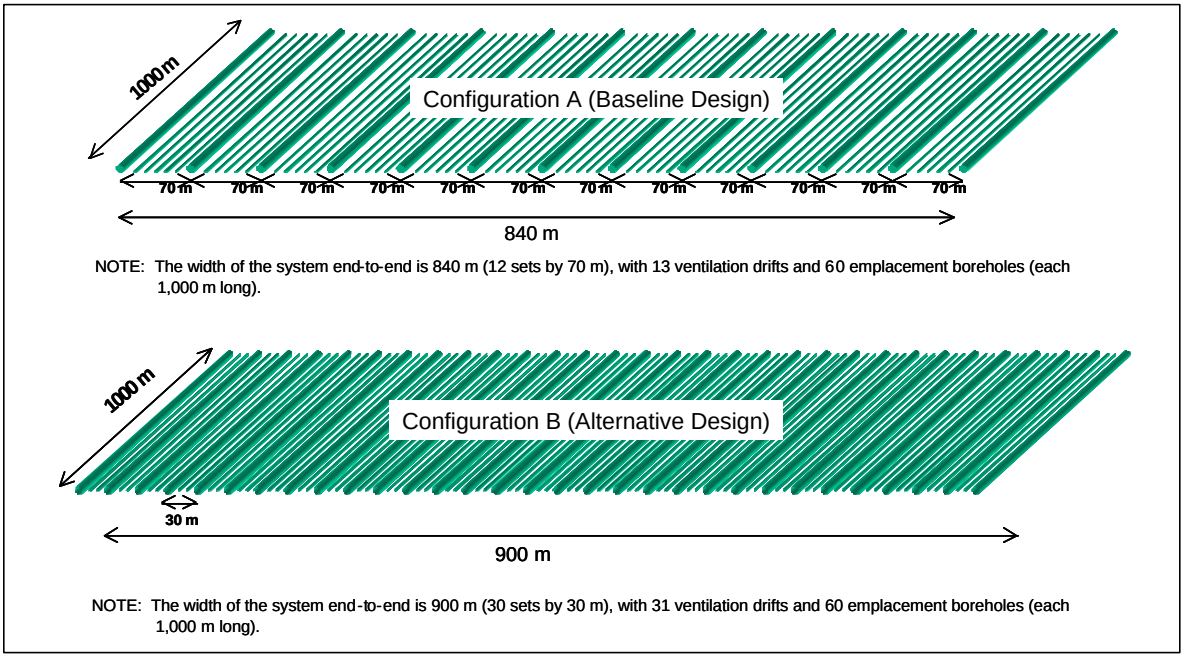

Figure 3
Schematic Diagram of Sections of the Conceptual Naturally-Ventilated Repository Showing the Total Space Requirement for Two Configurations

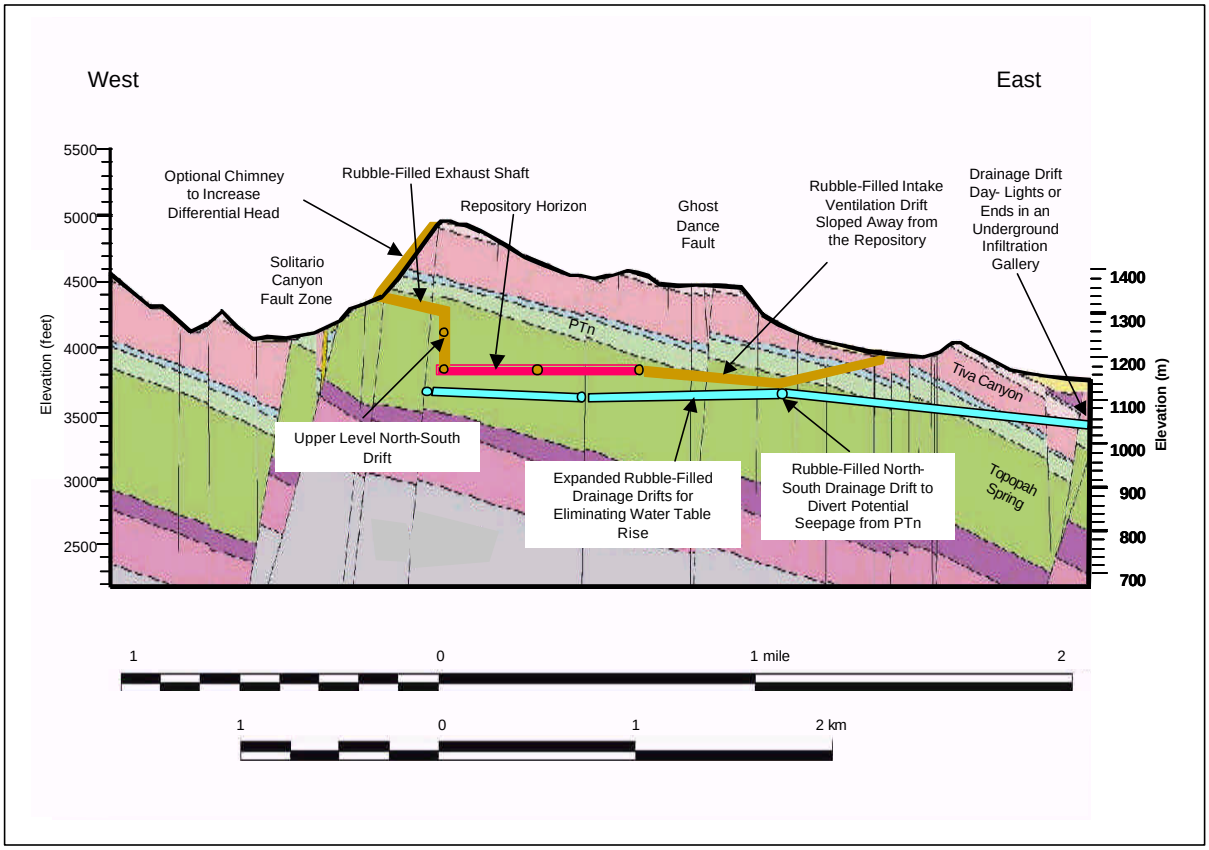

Source: Modified from DOE (2001a); refer to DOE (2001a, Figure 1-10) for detailed geologic description.

Figure 4
Simplified Cross Section of Yucca Mountain Showing the Conceptual Underground Ventilation and Potential Drainage System

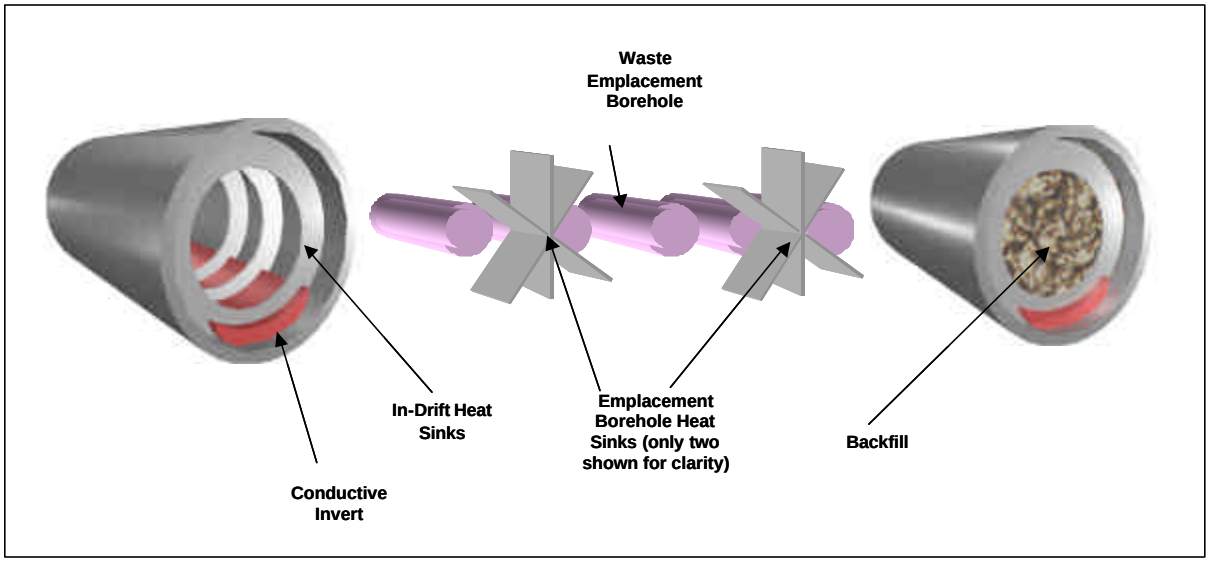

NOTE: Small, solid cylinders depict the waste packages.

Figure 5
Schematic Diagram of a Section of the Baseline (Configuration A) Conceptual Naturally-Ventilated Repository with the Rubble-Filled Drifts and Possible Heat Sinks

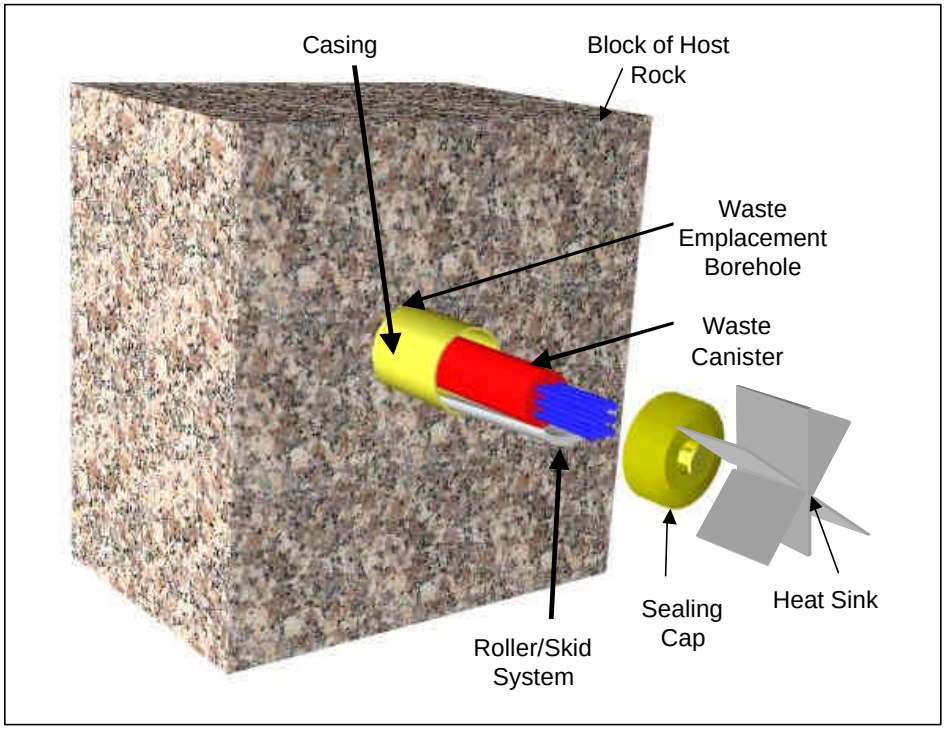

Figure 6
Schematic Diagram of the Conceptual Design of the Waste Emplacement Boreholes

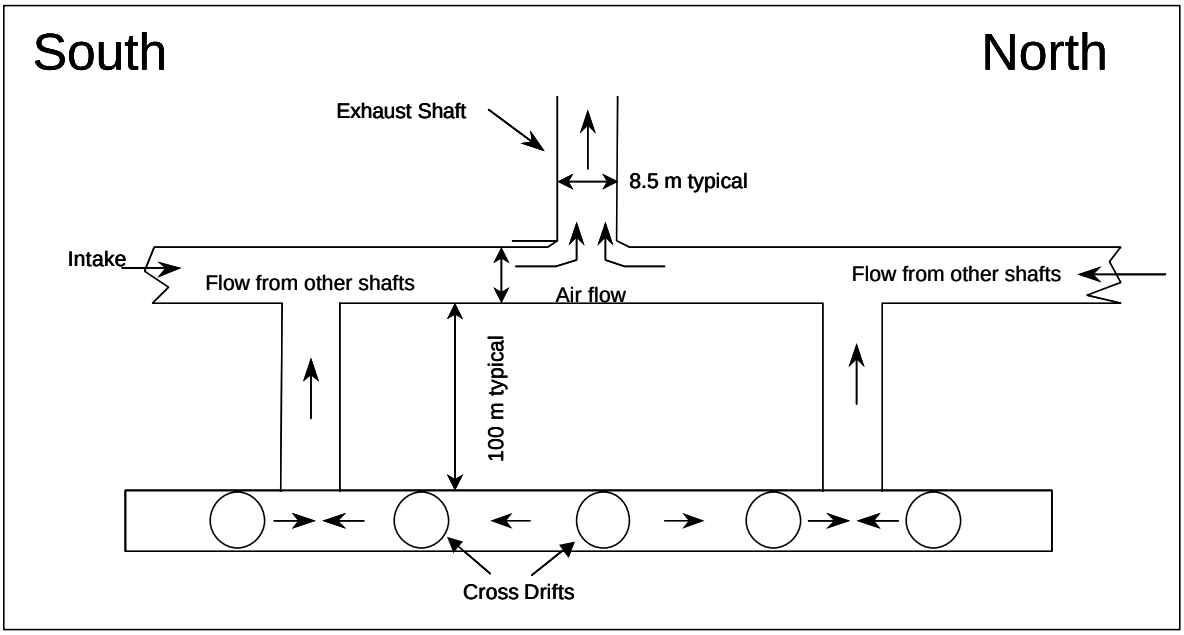

Source: Modified from Montazer (1998)

Figure 7
Cross-Sectional View of the Multi-Level Drifts and Shafts Concept

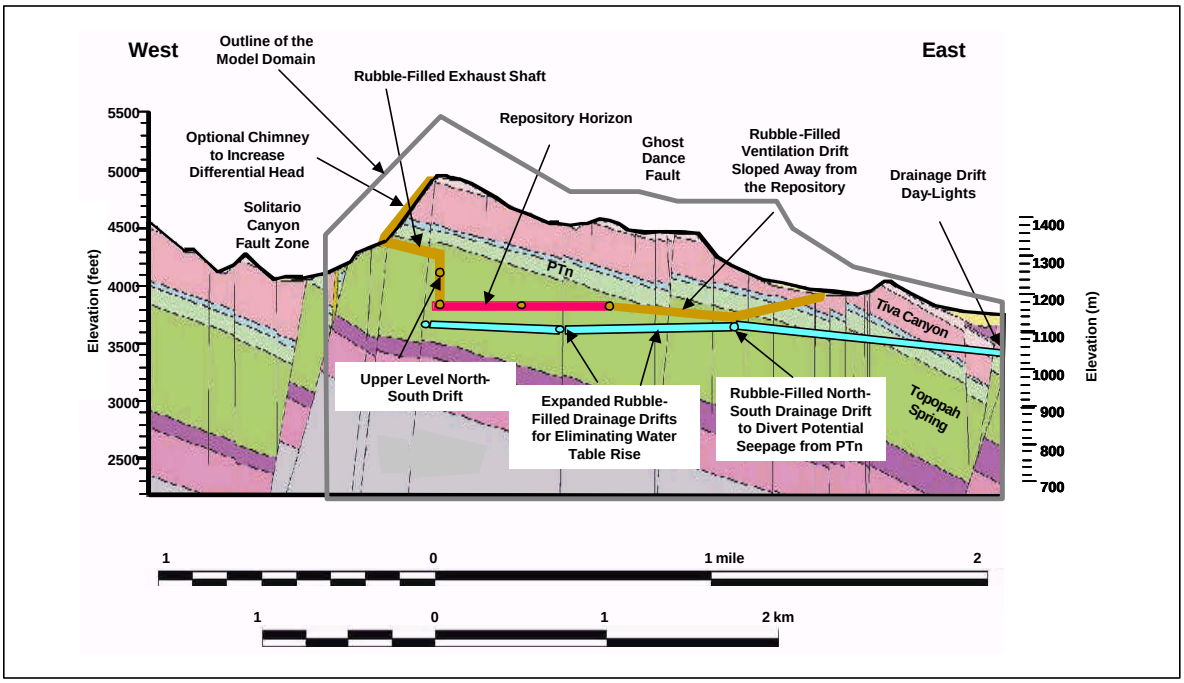

Source: Modified from DOE (2001a); refer to DOE (2001a, Figure 1-10) for detailed geologic description.

Figure 8
Simplified Cross Section of Yucca Mountain Showing Major Components of the Permanently-Ventilated Repository and the Domain of the Proposed Model Mesh

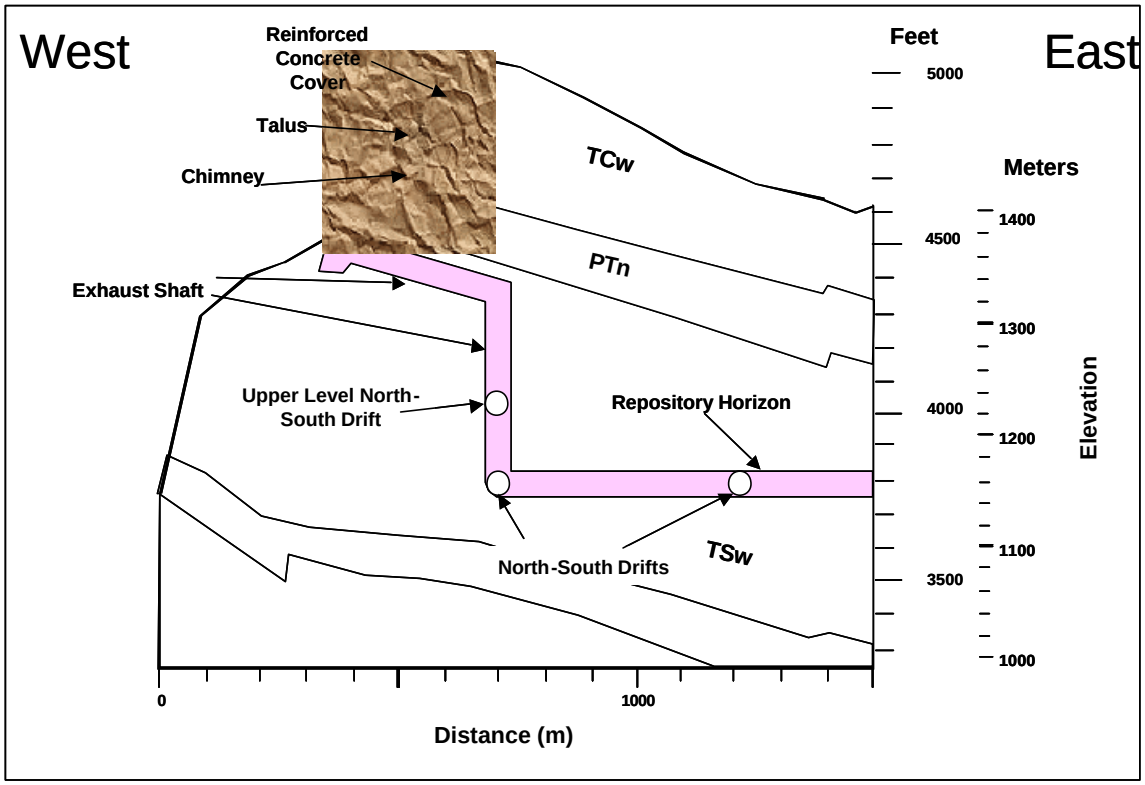

Figure 9
Cross-Sectional View of an Exhaust Shaft and a Chimney

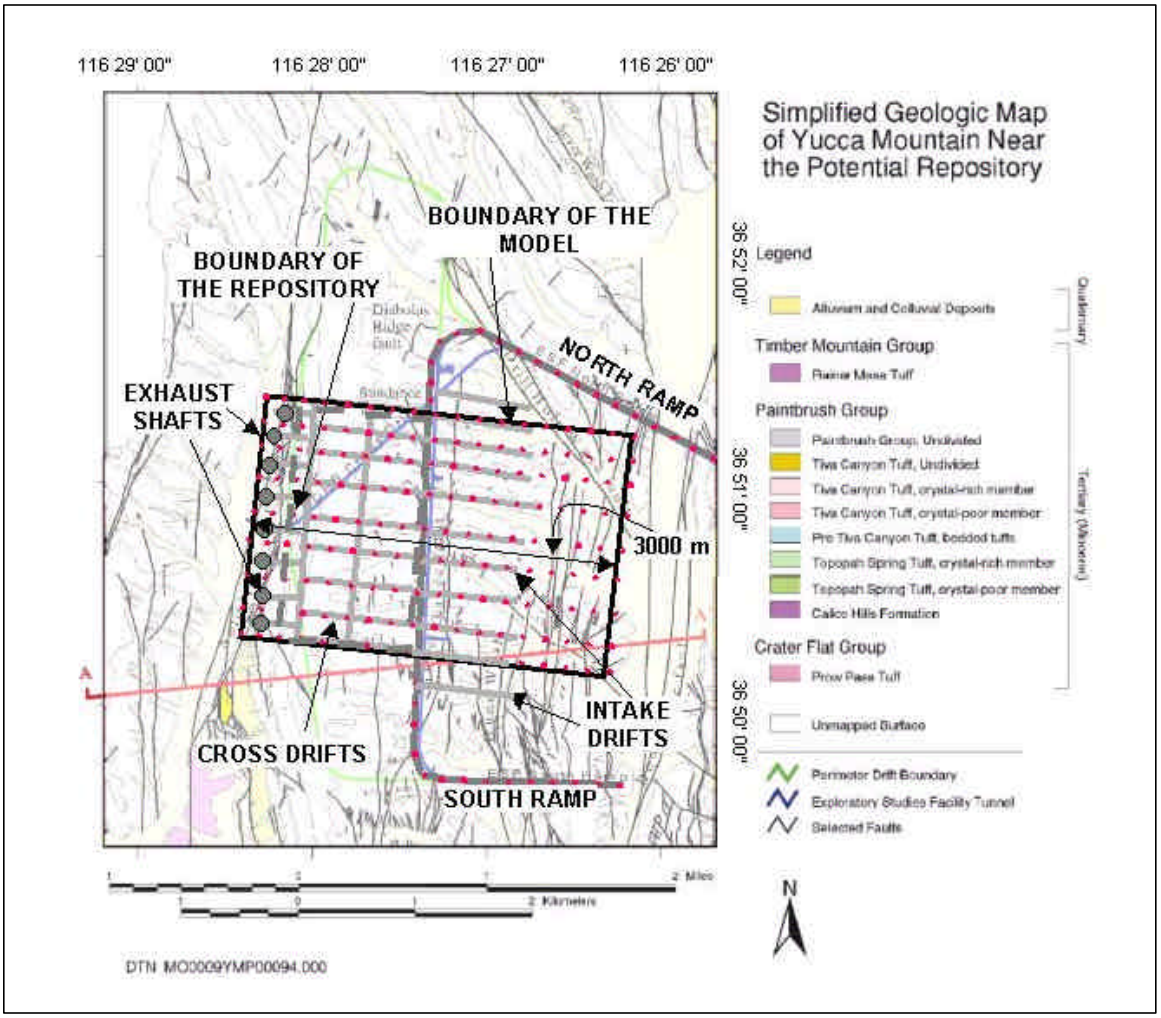

NOTE: Waste emplacement boreholes are not shown.

Figure 10
Plan View of the Approximate Distribution of Model Mesh Nodes within the Proposed Model Domain Overlaid on Top of the Simplified Geologic Map

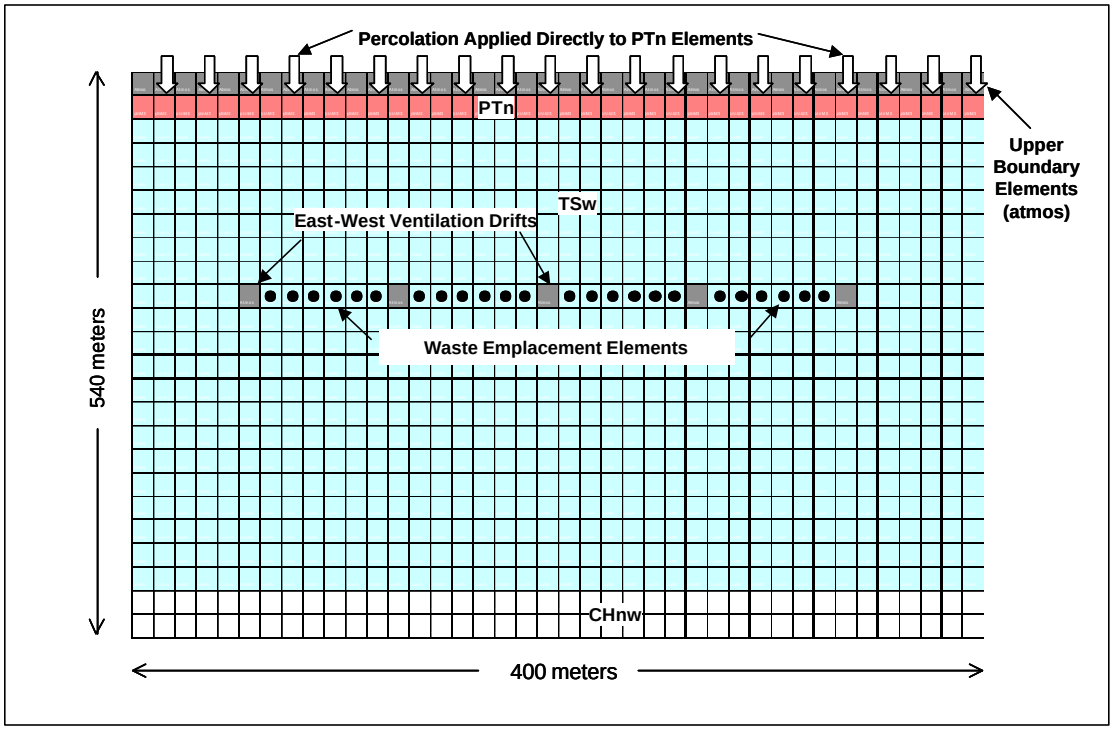

Figure 11
Refined North-South Mesh 4 for Preliminary Analyses of the Conceptual Underground Ventilation

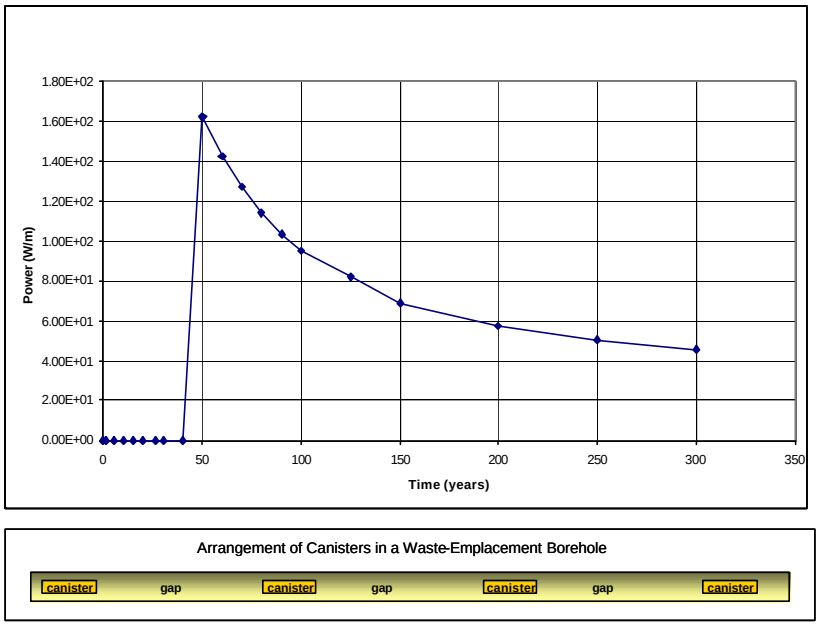

Figure 12
Heat Load History for a Simulation Using North-South Mesh 4 with Five Heaters between Ventilation Drifts and 25% of Full Heat Load Applied after 50 Years

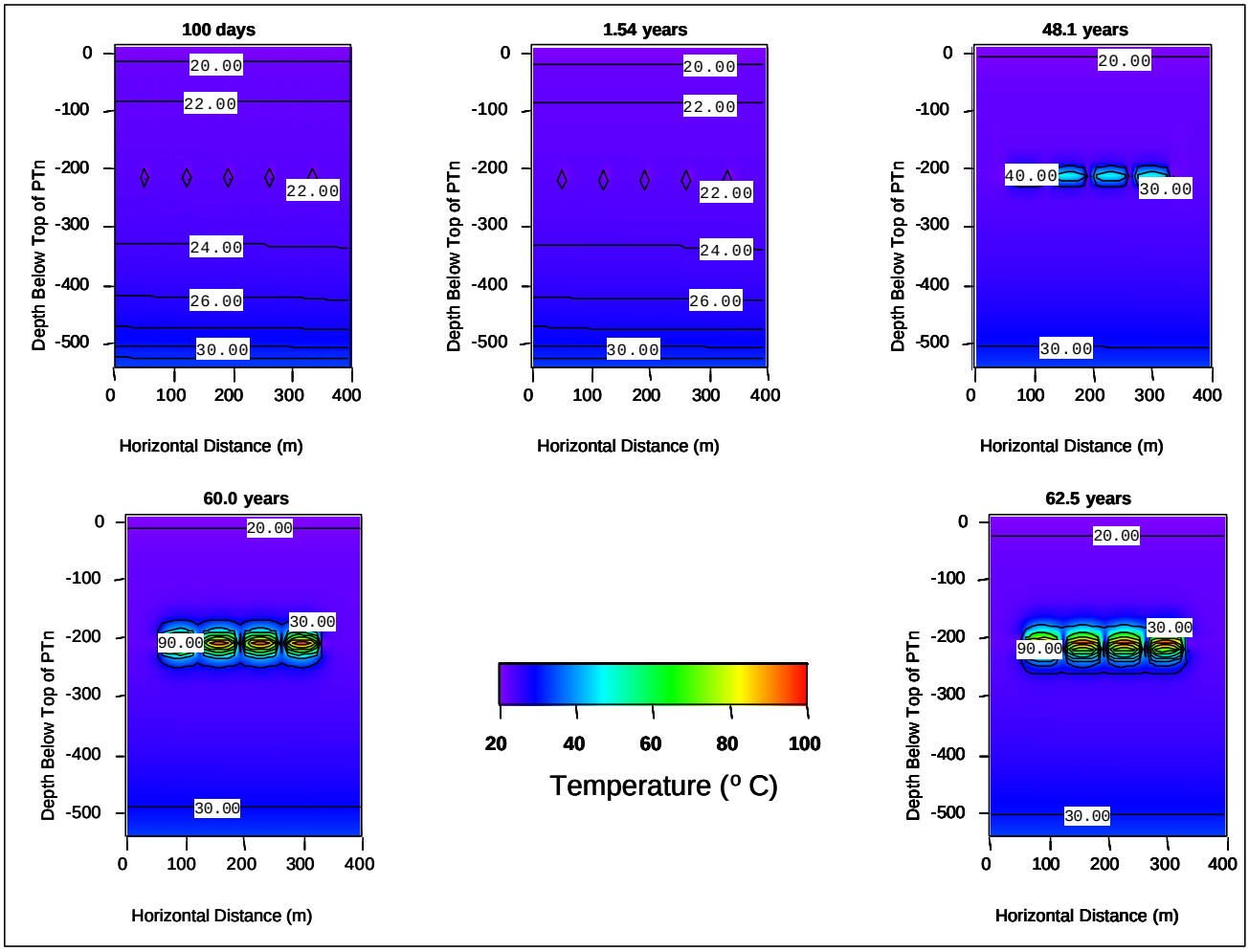

Figure 13
Distribution of Temperature for the Simulation Using Fine Mesh 4 with Six Heaters between Drifts and 25% of Full Heat Load Applied after 50 Years

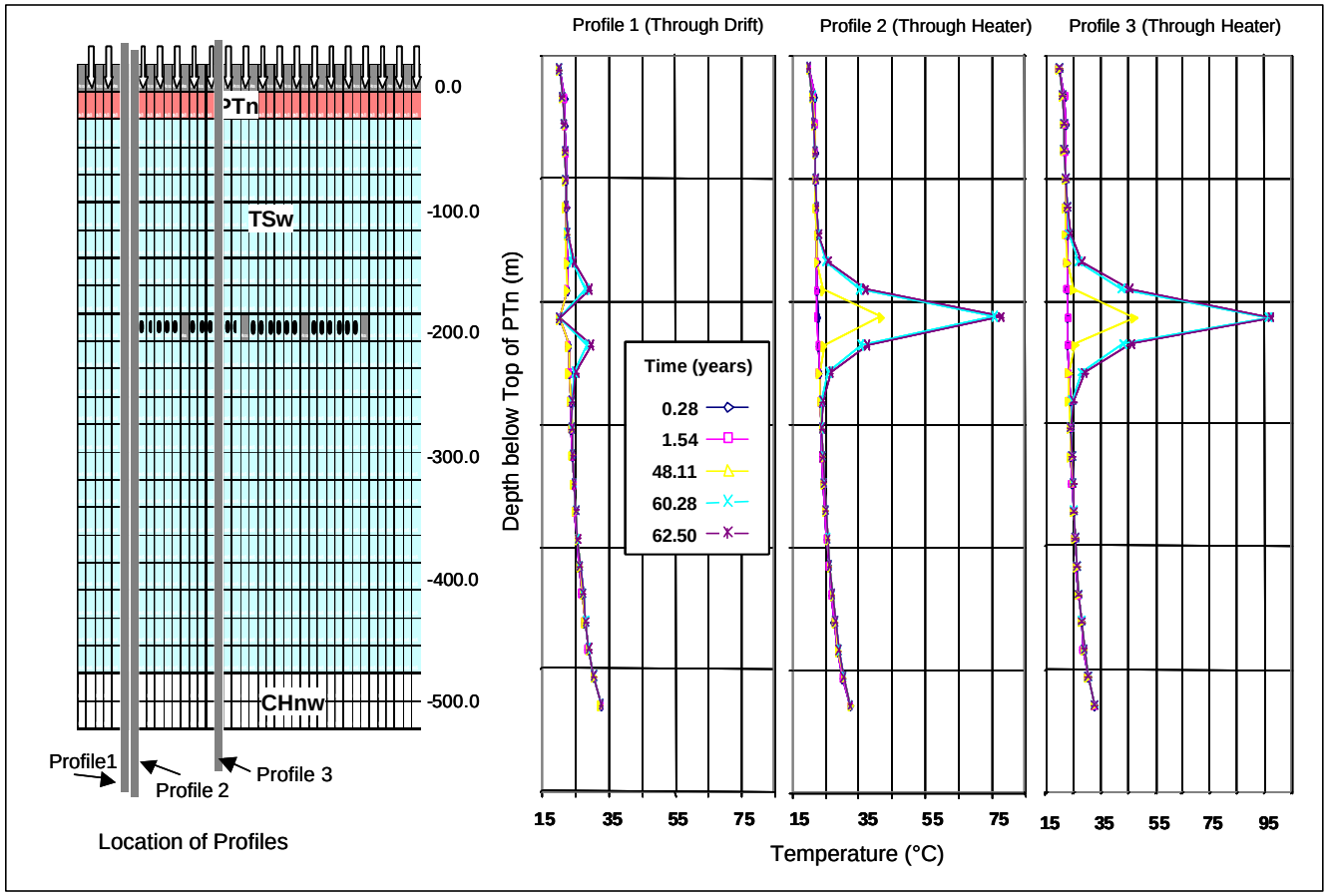

Figure 14
Profiles of Temperature for the Simulation Using North-South Mesh 4 with Five Heaters between Ventilation Drifts and 25% of Full Heat Load Applied after 50 Years

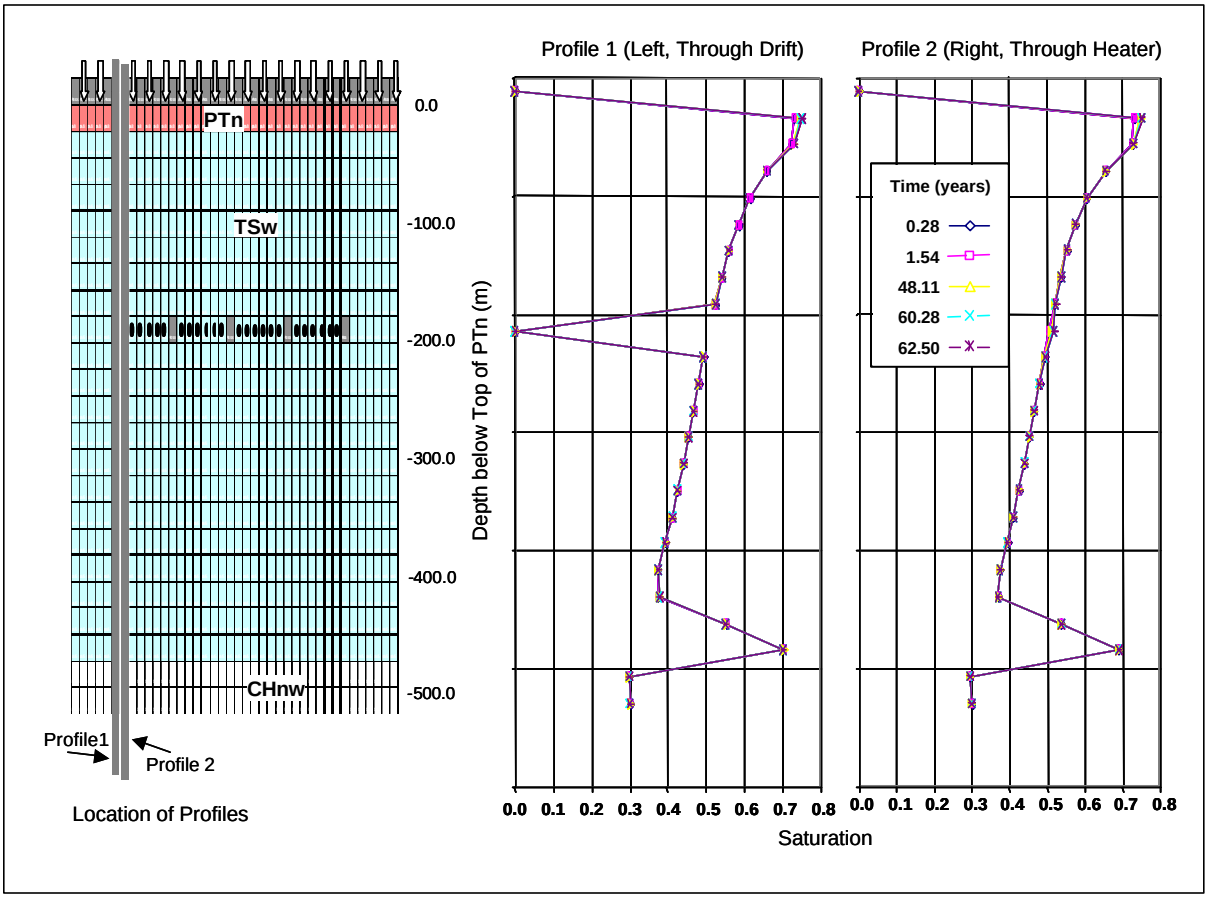

Figure 15
Profiles of Saturation for the Simulation Using North-South Mesh 4 with Five Heaters between Ventilation Drifts and 25% of Full Heat Load Applied after 50 Years

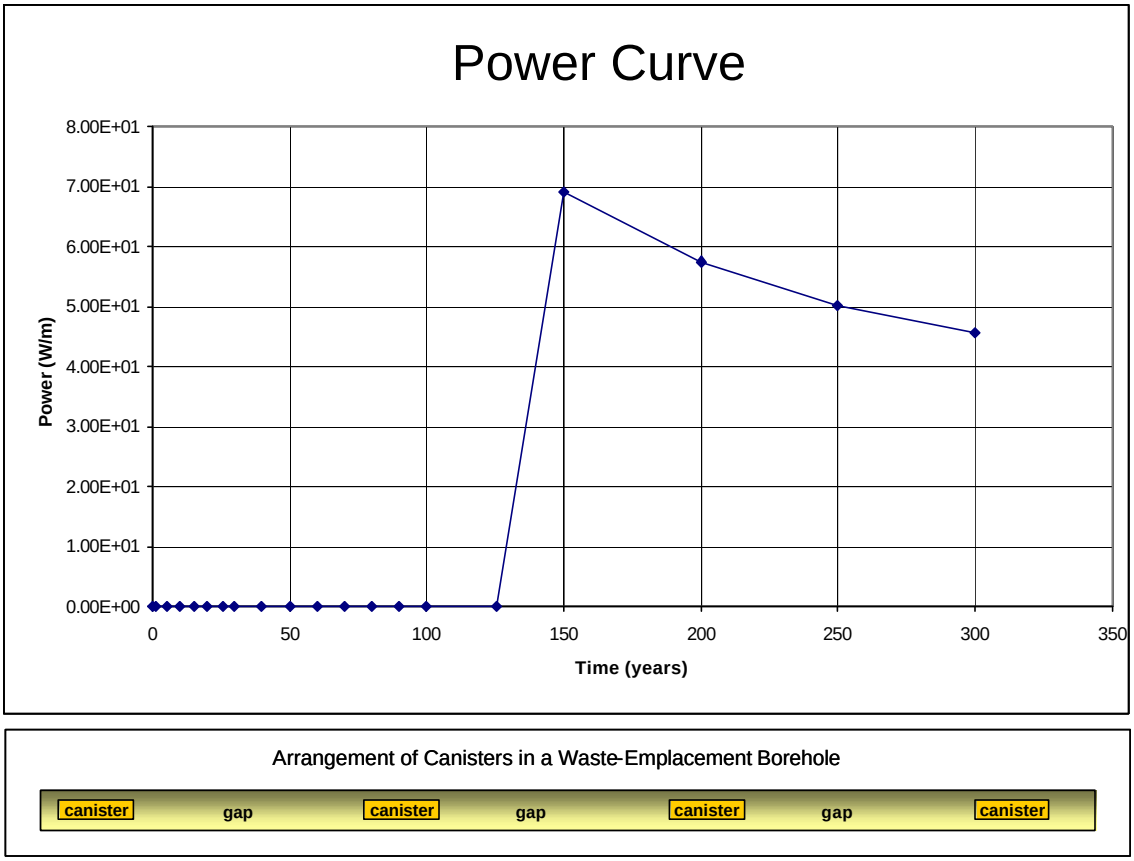

Figure 16
Heat Load History for a Simulation Using North-South Mesh 4 with Six Heaters between Ventilation Drifts and 25% of Full Heat Load Applied after 150 Years

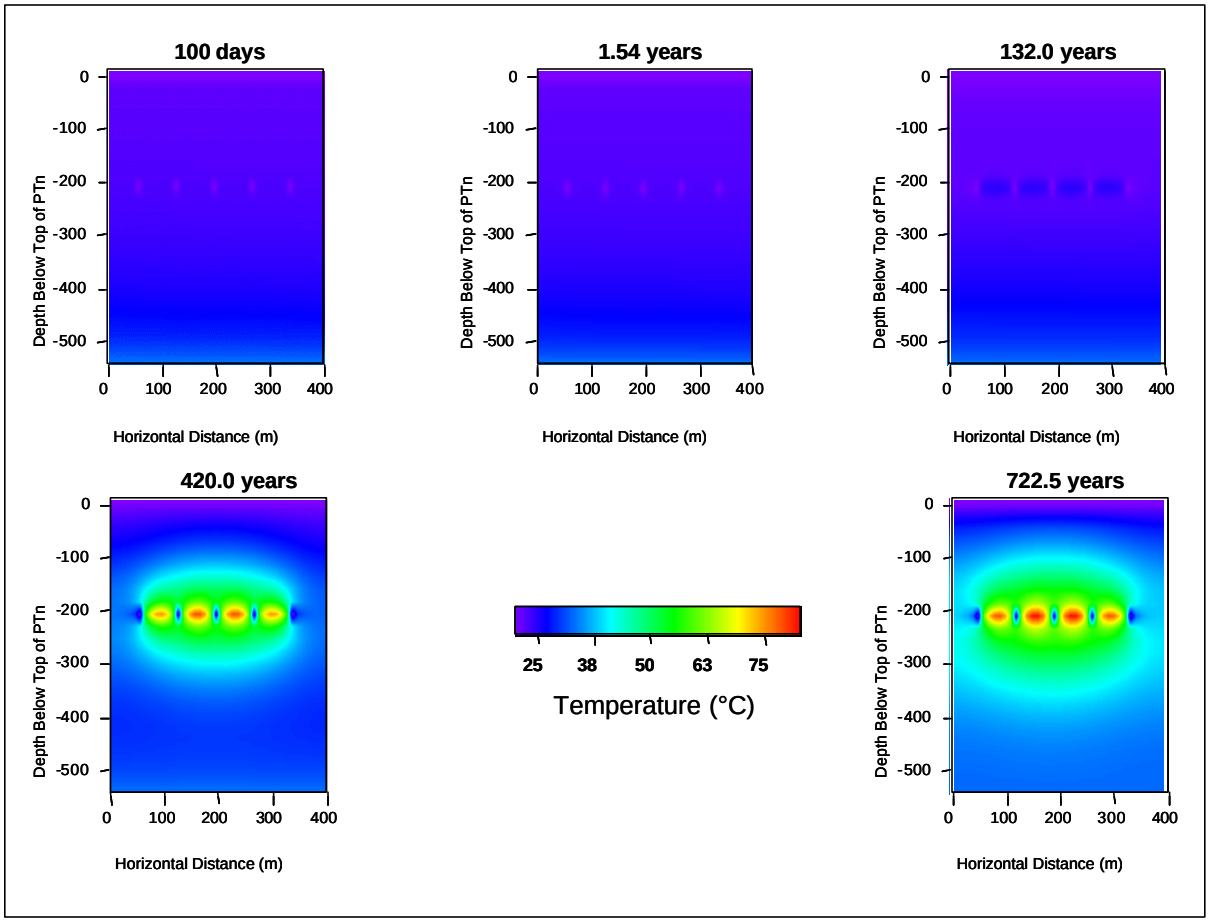

Figure 17
Distribution of Temperature for a Simulation Using North-South Mesh 4 with Six Heaters between Ventilation Drifts and 25% of Full Heat Load Applied after 150 Years

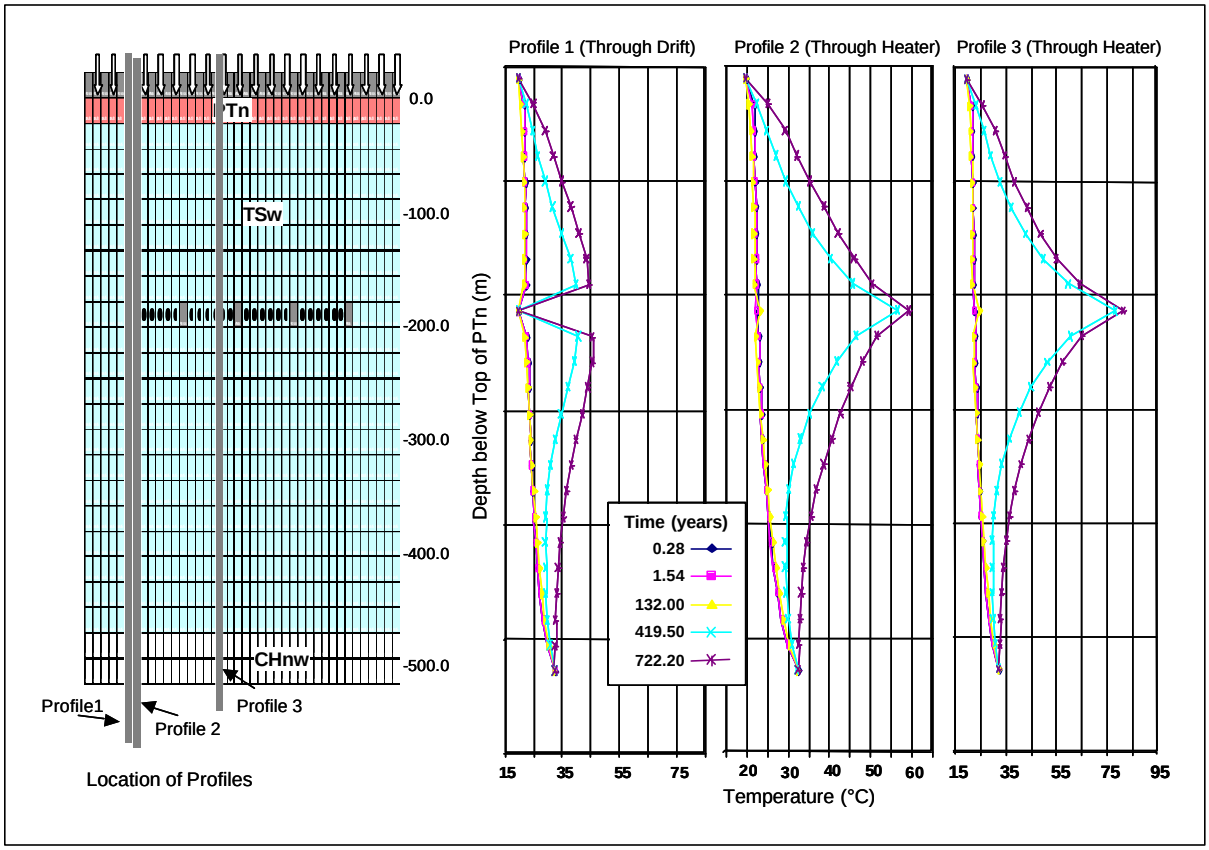

Figure 18
Profiles of Temperature for the Simulation Using North-South Mesh 4 with Six Heaters between Ventilation Drifts and 25% of Full Heat Load Applied after 150 Years

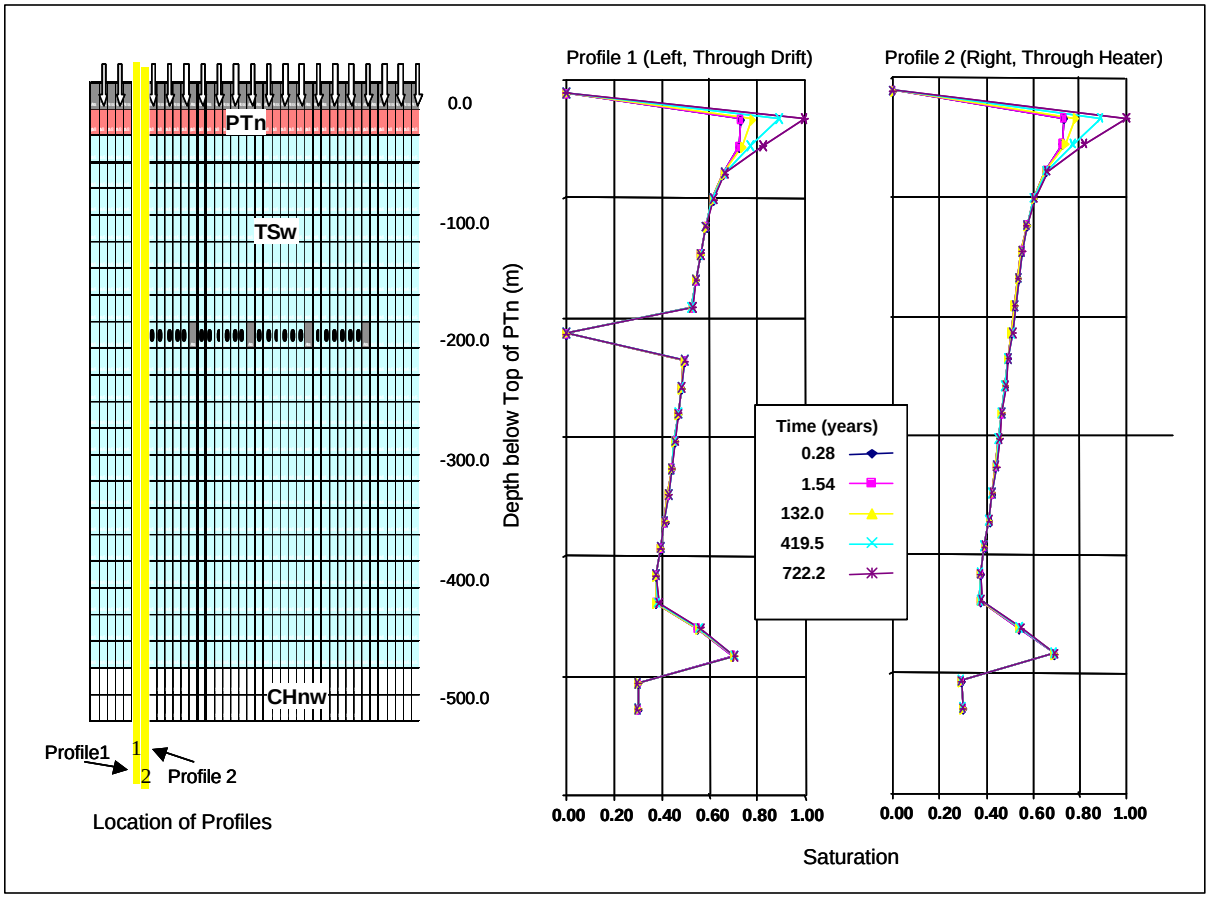

Figure 19
Profiles of Saturation for the Simulation Using North-South Mesh 4 with Six Heaters between Ventilation Drifts and 25% of Full Heat Load Applied after 150 Years

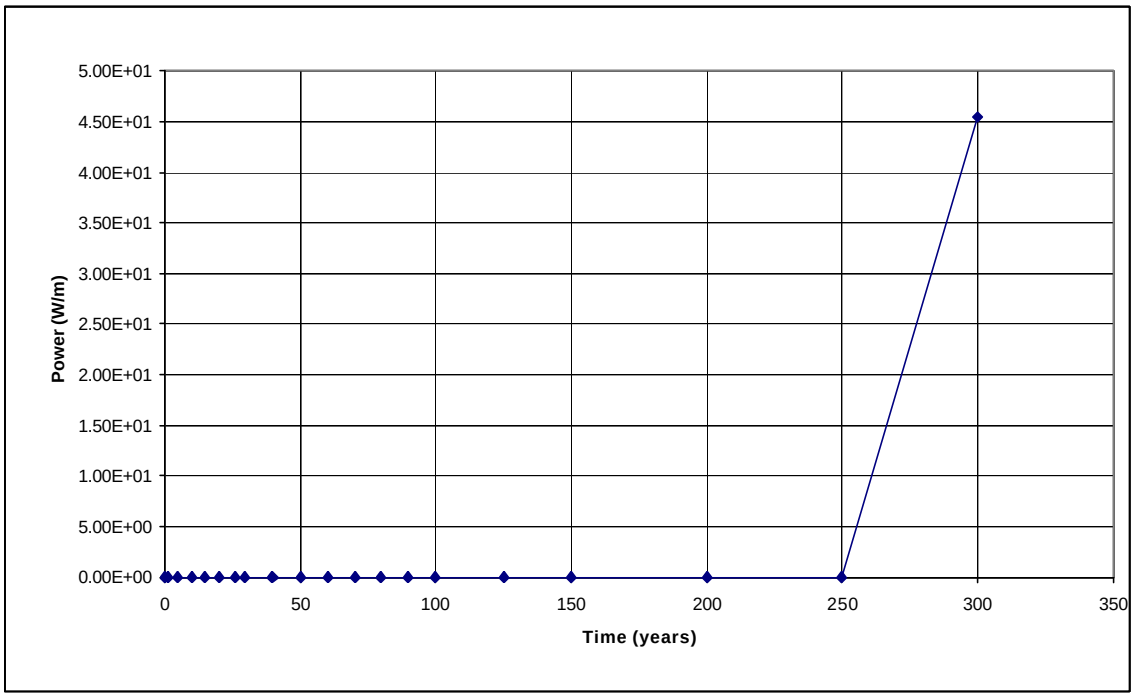

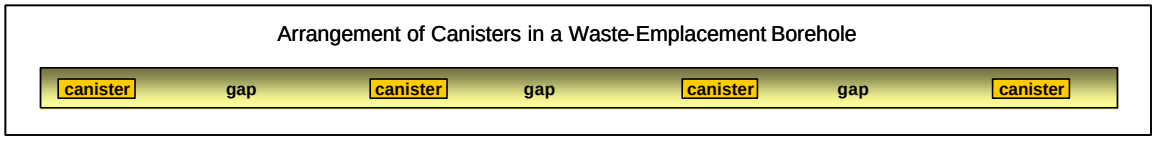

Figure 20
Heat Load History for the Simulation Using North-South Mesh 4 with Six Heaters between Ventilation Drifts and 25% of Full Heat Load Applied after 300 Years

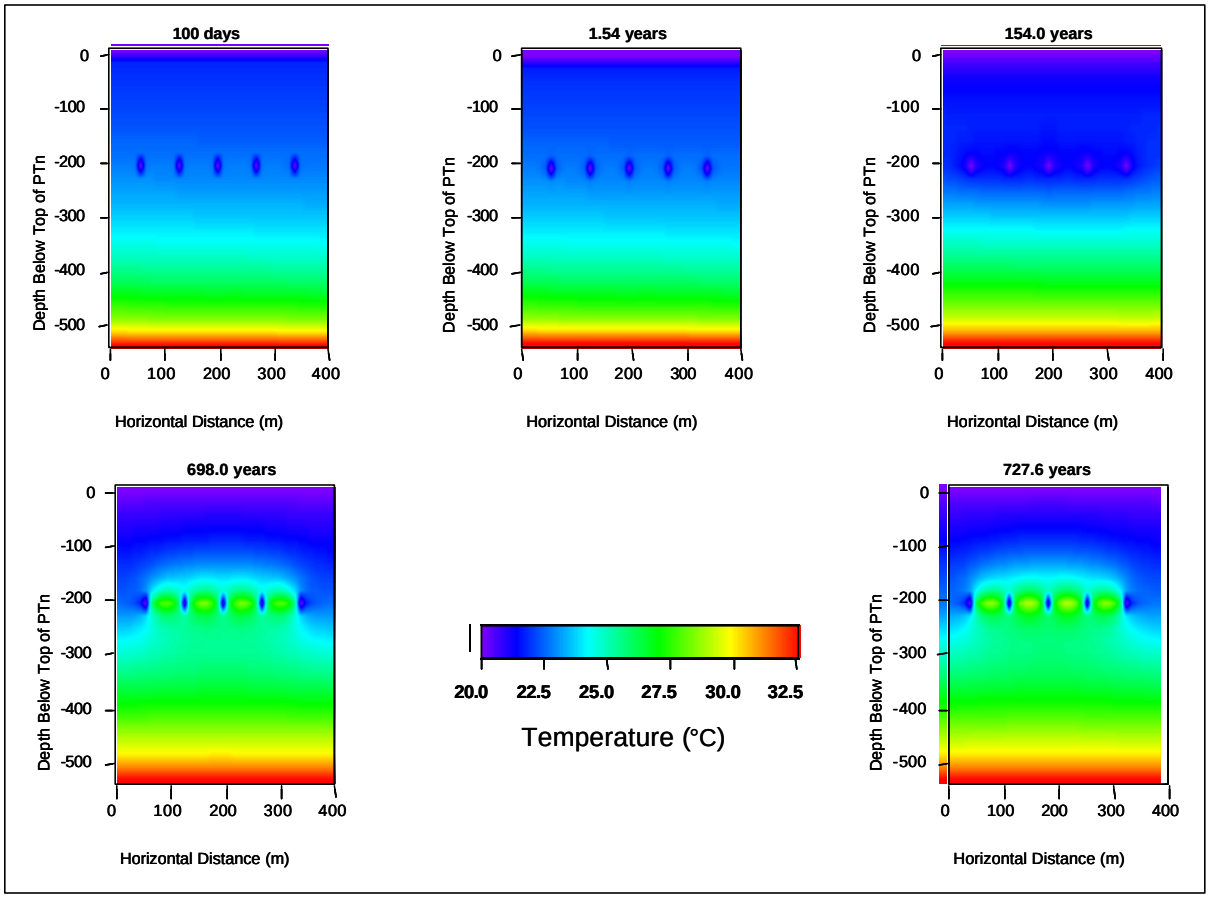

Figure 21
Distribution of Temperature for the Simulation Using North-South Mesh 4 with Six Heaters between Ventilation Drifts and 25% of Full Heat Load Applied after 300 Years

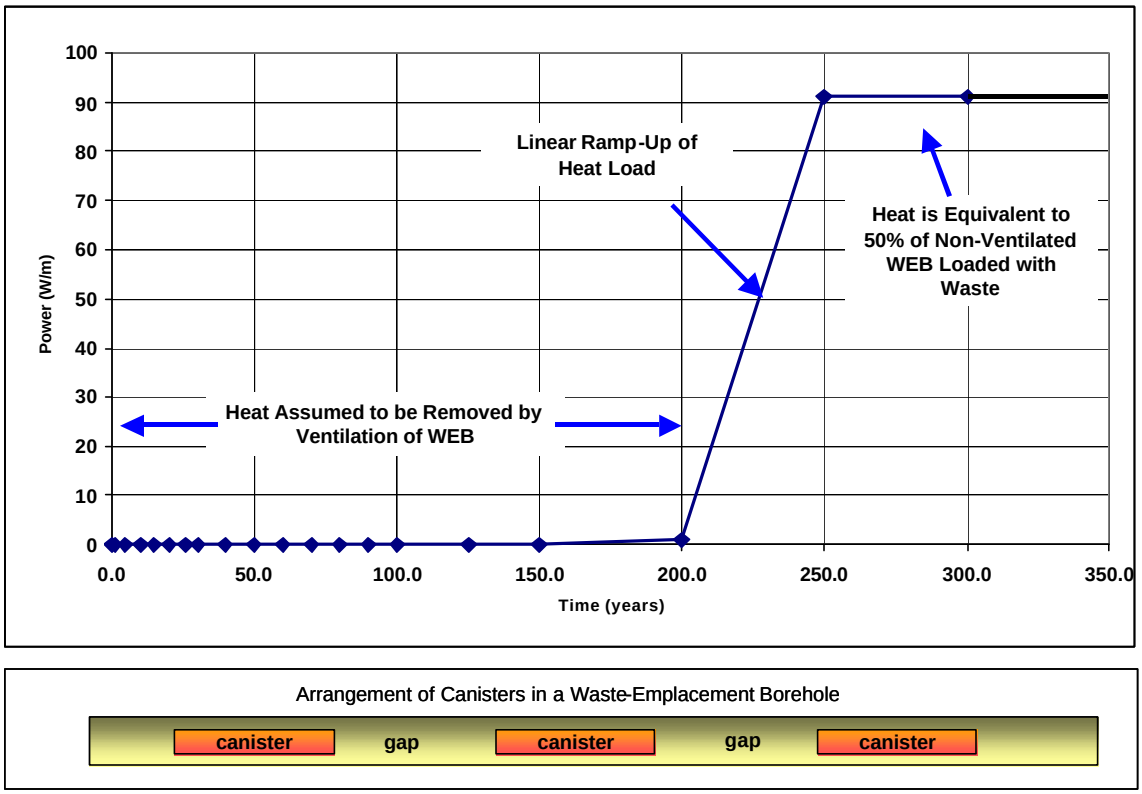

NOTE: WEB = waste-emplacement borehole

Figure 22
Heat Load History for a Simulation with Two Heaters between Ventilation Drifts and 50% of Full Heat Load Applied after 250 Years

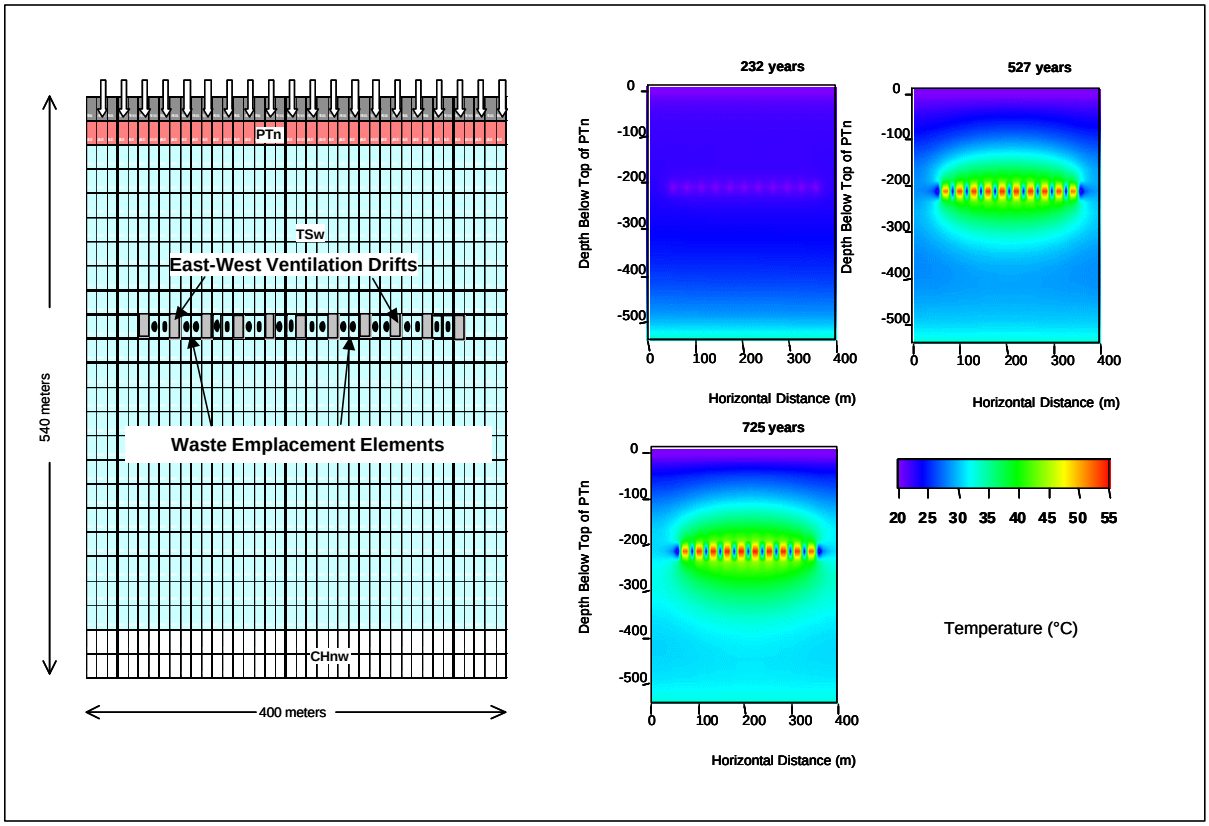

Figure 23
Distribution of Temperature for a Simulation with Two Heaters between Ventilation Drifts and 50% of Full Heat Load Applied after 250 Years

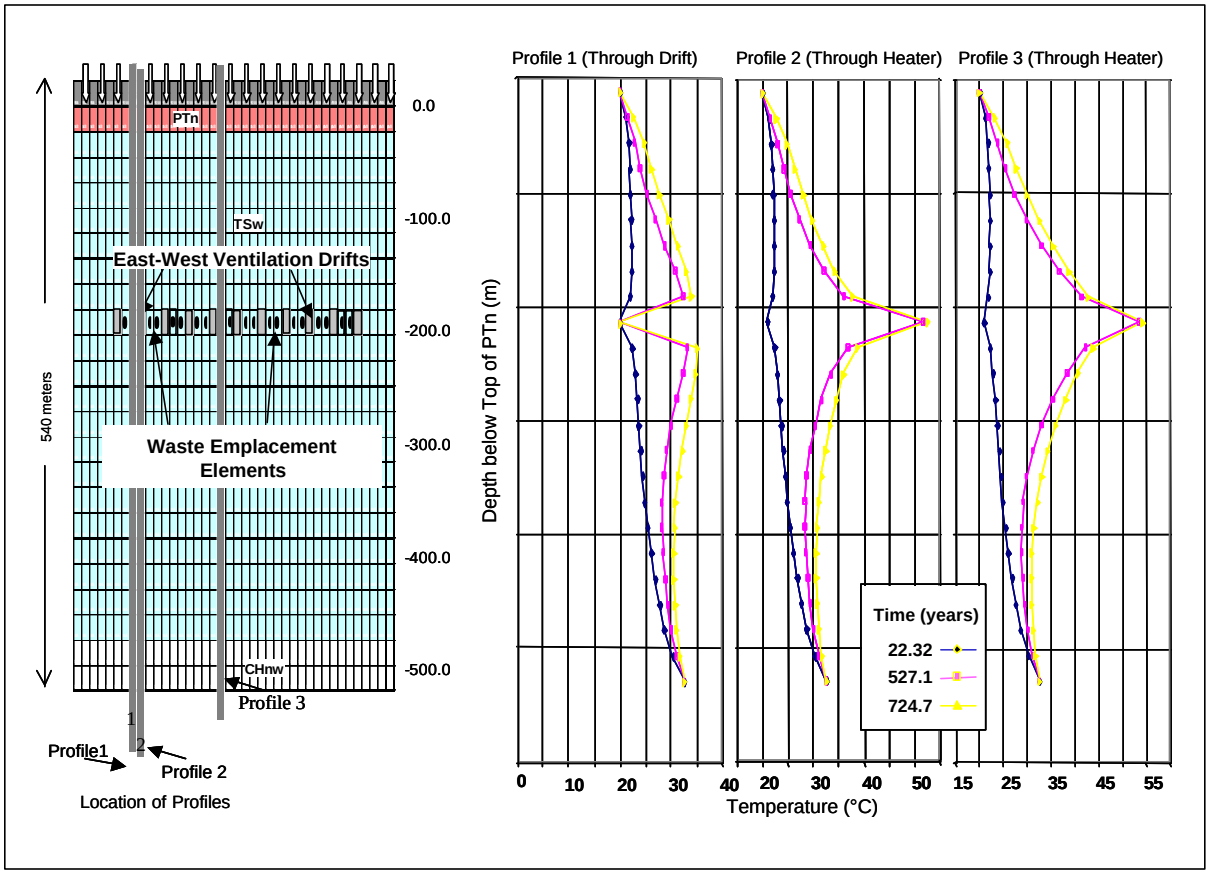

Figure 24
Profiles of Temperature for a Simulation with Two Heaters between Ventilation Drifts and 50% of the Full Heat Load Applied after 250 Years

TABLES

APPENDIX A
DESCRIPTION AND VERIFICATION OF A-TOUGH2 CODE

INTENTIONALLY LEFT BLANK

CONTENTS

FIGURES

TABLES

ACRONYMS AND ABBREVIATIONS

A-TOUGH2	Atmospheric TOUGH2
EOS	equation of state

INTENTIONALLY LEFT BLANK

DESCRIPTION AND VERIFICATION OF A-TOUGH2 CODE

BACKGROUND

A-TOUGH (MET, 1995; Montazer et al., 1994) is an atmospheric or open-air chamber simulation code based on TOUGH (Pruess, 1987) and V-TOUGH (Nitao, 1989) codes. A-TOUGH has been successfully tested with several simple and complicated problem sets (Montazer et al., 1994). The atmospheric module of A-TOUGH2 is the same as that of A-TOUGH. The only difference between A-TOUGH and A-TOUGH2 is in the simulation of the porous media, as described in Pruess et al. (1999). TOUGH2 offers several equations of state (EOS) to choose from. In A-TOUGH2, the EOS modified is EOS7R. The EOS7R module of TOUGH2 is designed to simulate multiphase flow and transport of water, brine, air, parent-daughter radionuclides, and volatile organic compounds. This capability is inherited by A-TOUGH2. EOS7R provides certain improvements, but also imposes some inherent restrictions on A-TOUGH2 that are discussed below.

A-TOUGH2 was developed from TOUGH2 to simulate the transport of air, vapor, and heat through an atmospheric boundary layer coupled with the transport of moisture, air-vapor mixture, and heat through porous or fractured media. The three-dimensional nature of the code allows simulation of rough terrain and heterogeneous subsurface conditions encountered at sites such as Yucca Mountain, Nevada. The allowable range of temperature (-50°C to 200°C) and relative humidity (0 to 100 percent) values permit the simulation of complex processes, such as condensation in fractures during the winter season. A-TOUGH2 can also be used to predict the effects of flow of air in ventilation shafts and tunnels in underground facilities. Moisture conditions in both fractured and porous media can be included in simulations.

In this appendix, only the verification of the A-TOUGH2 will be presented. The set of problems used for verification and validation are the same as those used for A-TOUGH. The input structures for the porous media portion of the code are identical to those described in Pruess et al. (1999). The input structures for the atmospheric portion are identical to those described in MET (1995) for A-TOUGH. For these reasons, no new user's guide was generated for A-TOUGH2. In the following sections, the theory for the development of A-TOUGH and A-TOUGH2 is briefly described. More details are provided in MET (1995) and Pruess et al. (1999).

The problem of interfacing the atmosphere with the surface soil layer is that the flow of air in the atmosphere is turbulent even during the calmest days (Bird et al., 1965; Brutsaert, 1982). The transport of vapor in the atmospheric boundary layer near the ground surface is rapid and may be approximated using eddy diffusion for both the mass and energy transfer coefficients. This simplification has been used by others to describe the mass and energy transfer across the boundary layers in turbulent conditions (Bird et al., 1965; Peixoto and Oort, 1992; Fritchen and van Bavel, 1962).

Atmospheric fluctuations result in massive amounts of air moving into and out of subsurface environments. In circumstances where the atmosphere has low humidity, the amount of moisture that can be transferred to the atmosphere during outflow of this air could be substantial. In addition, when air moves across surficial material with different properties and different topographies (rough terrain), the vapor flux varies. This variation in moisture flux along the

surface of the boundary layer can cause significant variations in the humidity and thermal energy of the moving air.

In A-TOUGH2, the coupling between atmospheric nodes and soil nodes is accomplished through the use of eddy diffusivity coefficients for both vapor and heat transfer. This allows discretization of the atmosphere as a different material property in the simulation domain.

The following section summarizes the principles used to simulate the transfer of vapor and heat between the soil and atmosphere. Figure A1 is a simplified diagram depicting the connection between an atmospheric element and a surface element. The two elements have significantly different material properties and different governing process equations.

The transport of vapor from the molecular sublayer to the atmosphere is a function of surface roughness, wind shear, and thermal stratification, as well as the humidity (or vapor concentration) gradient. Details of the processes and formulations are provided in the literature (Brutsaert, 1982; Stannard, 1993). The rate of vertical vapor transfer (or evaporative flux) is given by:

$$q_{evap} = -D^*_{atm} \left. \frac{\partial r_{vw}}{\partial z} \right|_{z_0} \qquad \text{(Eq. A-1)}$$

and

$$r_{vw}(z) = r^*_{vw}(z) h(z) \qquad \text{(Eq. A-2)}$$

where, r_{vw} is the vapor density, r^*_{vw} is the saturated-vapor density, and h is the humidity. The symbol z denotes the vertical distance above the ground surface. Equation A-1 is similar to Fick's law of diffusion except that the molecular diffusion coefficient is replaced with D^*_{atm}, the eddy diffusivity. Eddy diffusivity is a time-dependent parameter and varies with temperature and wind speed.

The transfer of heat across atmospheric layers with turbulent flow is governed by the following equation (Peixoto and Oort, 1992):

$$F_{SH}(z) = K_H \, r_a c_p \frac{\partial T}{\partial z} \qquad \text{(Eq. A-3)}$$

where F_{SH} is the sensible heat flux, K_H is the eddy diffusion coefficient for heat (which is commonly set equal to D^*_{atm} [Peixoto and Oort, 1992]), r_a is the density of air, c_p is the atmospheric specific heat at constant pressure, and T is the temperature. Therefore, thermal conductivity (K_{atm}) is calculated for the atmospheric layers as:

$$K_{atm} = D^*_{atm} r_a c_p \qquad \text{(Eq. A-4)}$$

A major modification of TOUGH2 to produce A-TOUGH2 is the replacement of the vapor-diffusive flux term with Equation A-1 for the atmospheric elements. That is:

$$-D_{va}\rho_g \nabla X_g^w = q_{evap} = -D_{atm}^* \frac{\partial \rho_{vw}}{\partial z} \quad \text{(Eq. A-5)}$$

where D_{va}^0 is air/vapor mixture diffusion coefficient, $?_g$ is gas-phase density, and X_g^w is the mass fraction of the gas phase.

The horizontal transfer in the atmosphere occurs primarily by advective transport with the air. Therefore, whenever the vertical transfer between atmospheric and soil elements is calculated, eddy diffusivity is used to calculate the diffusive flux and added to the advective term. The advective transport in all directions, whenever atmospheric elements are involved, is calculated in the normal way except that an appropriately large value of gas permeability is used for the atmospheric element. With appropriate gas permeability values for the atmospheric elements and the eddy diffusivity, turbulent horizontal transport of vapor can be simulated.

Eddy diffusivity is a dynamic parameter, changing with wind speed, air temperature, and other factors. Therefore, in order to couple subsurface processes with atmospheric processes, the eddy diffusivity and thermal diffusivity parameters must be varied dynamically, in addition to the soil-atmosphere boundary conditions.

For atmospheric simulations, the relative permeability function Type 2 of TOUGH is used (Pruess, 1987):

$$k_{rl} = S_l^{100} \quad \text{(Eq. A-6)}$$

$$k_r = 1 \quad \text{(Eq. A-7)}$$

where k_{rl} is the relative liquid permeability of the atmospheric node, S_l is the liquid saturation (which is always set to zero or a very small number for the atmospheric element), and k_r is the relative air permeability of the atmospheric node. Therefore, the relative liquid permeability of the atmosphere is set to a value near zero (by raising a very small number to the power 100). The relative air permeability is always equal to one. TOUGH2 is also modified to maintain the atmospheric node in single-phase mode at all times in A-TOUGH2. Condensation is allowed to occur in the surface soil nodes if warm and humid atmospheric air enters a cooler soil.

The numerical discretization methods used in TOUGH2 are largely preserved in A-TOUGH2. Details of the numerical approximation used in TOUGH2 are provided by Pruess et al. (1999), Pruess (1987), and Nitao (1989).

Boundary conditions are set in A-TOUGH2 in the same manner as TOUGH2 by using boundary nodes. In addition, in A-TOUGH2, when the ATMOS control code is used, the nodes with

volumes larger than 0.5×10^{30} m^3 are set as atmospheric boundary nodes. The boundary values are provided in an external file that contains the atmospheric parameters (temperature, pressure, relative humidity, and eddy diffusivity) as a function of time. Otherwise, the atmospheric types of nodes are treated as internal atmospheric nodes with eddy diffusivity as the vapor-mass and sensible-heat transport coefficients, and are allowed to interact with the soil nodes.

Sources and sinks are used at the boundaries to implement a flux boundary condition (Neumann type, e.g., rainfall and solar radiation). Rainfall is introduced as a water-mass source into the upper soil layer. Solar radiation is also defined as a heat source at the upper soil layer.

CODE MODIFICATION

Modification of the V-TOUGH to A-TOUGH code is documented in detail in MET (1995). The procedures used to produce A-TOUGH2 were similar, except that the modifications were made to corresponding modules of TOUGH2. In TOUGH2, the EOS7R was used for the EOS. All changes in the code were documented.

CODE COMPILATION

Codes were compiled using Fortran PowerStation, version 5.0, of the Digital Electronic Corporation (DEC, now Compaq Corporation). DEC Alpha processor was used as the platform for compilation and calculations.

CODE VERIFICATION

For verification, A-TOUGH2 results were compared with results of a simplified, one-dimensional, two-cell (Figure A1) mass balance analytical model in a study that involved varying eddy diffusivity, capillary pressure, humidity, and temperature (MET, 1993). Table A1 shows the results of this model compared with the results of A-TOUGH2. The absolute value of the largest relative error was found to be 58.8. For a majority of cases, the relative error was smaller than 0.3. Relative errors smaller than 0.5 were acceptable for the purposes of this project. The large errors (greater than 10) are associated with the use of a relative humidity of 1.0 (100 percent vapor saturated air) for both the atmospheric and soil nodes under isothermal conditions. At such conditions, the vapor pressure gradient between the atmospheric and soil elements should be zero, which cannot be accommodated numerically by the model. Therefore, the vapor flux calculated is very small (near zero), resulting in large calculated relative error. These conditions are not expected to occur during the simulations in this project. During most of the simulation time periods, the state conditions between the atmospheric and soil elements will be substantially different.

CODE VERIFICATION WITH PREVIOUS VERSION OF A-TOUGH

Because A-TOUGH has been extensively used and debugged, a series of simple problems were used to compare the results of A-TOUGH2 with A-TOUGH. These problems are set as one-, two-, and three-dimensional nodes with one simple atmospheric node. The purpose of these example problems was to verify that implementation of the atmospheric module into TOUGH2 produced the same results at A-TOUGH.

The one-dimensional problem was set to examine heat and fluid transport through a column of soil under summer atmospheric boundary conditions with varying amounts of precipitation, humidity, temperature, and solar radiation. It consisted of five elements stacked vertically in a column to a total height of 4.25 m. The soil consisted of four elements with material properties of silty sand, clay, and pea gravel. The top node was 2 m of atmosphere. The column was 2 m long and 1 m wide in the horizontal cross section. Details of the problem setup are provided in MET (1995).

The two-dimensional problem consisted of four of the one-dimensional columns put together side by side. The three-dimensional problem consisted of three of the two-dimensional slices put together in the third dimension.

The results of simulations were almost identical in all three cases for both A-TOUGH and A-TOUGH2. The only problem identified was the inability of the EOS7R module in reducing the saturation level below 0.01 percent. Using a different EOS available for the TOUGH2 package can alleviate this limitation. For the purposes of this project, this limitation is acceptable because rocks with saturation less than 0.01 are considered dry. At this saturation level, the eddy diffusivity between the rock and the air approaches that of the binary diffusion coefficient of an air-vapor mixture, resulting in small mass and heat transfer coefficients.

CODE VALIDATION

Code validation in this appendix refers to the comparison of the results of a particular aspect of the physical processes simulated by the code with the results of a controlled experimental setup.

A-TOUGH2 simulation results were compared with the field data reported by Passerat de Silans et al. (1989). The field data presented by these authors were collected from a 3,600-m^2 plot that extended to a depth of 80 cm. The vertical section consisted of three layers:

1. A barren silty-sand surface layer (crust) extending to a depth of 0.5 cm
2. A clayey silt layer extending to a depth of 30 cm
3. A second clayey silt layer extending to a depth of 80 cm.

The primary input parameters for this one-dimensional simulation were wind velocity, ambient air temperature, and atmospheric humidity. The calculated eddy diffusivity, the measured air temperature, and wind velocity as reported by these authors is shown in Figure A2.

Hourly variations in the atmospheric pressure, ambient air temperature, atmospheric humidity, solar flux, and atmospheric radiation were simulated for six days. It was assumed that no precipitation occurred during the six-day simulation period as reported by Passerat de Silans et al. (1989).

The measured and simulated volumetric moisture contents at various depths versus time are shown in Figure A3. The measured and simulated volumetric moisture contents increased with depth and varied from roughly 15 to 30 percent. A-TOUGH2 predictions were in reasonable agreement with measured values throughout the profile. Part of the reason for the slight discrepancy is attributed to the uncertainty in the soil parameters presented in graphical form by

Passerat de Silans et al. (1989). Simulated values were within 10 percent of measured values for depths below 2 cm. Simulated values were within 25 percent of the measured values for a depth of 1 cm below the ground surface.

The measured and simulated values for cumulative evaporation versus time are shown in Figure A4. Evaporation as predicted by the commonly-used Penman equation is also shown (Penman, 1948). The measured and simulated vapor flux increases monotonically from 0 mm (at the start of the experiment) to approximately 15 mm at the end of the experiment. Simulated evaporative flux closely agrees with measured values and the modeled values reported in the literature, while the Penman equation tends to overestimate evaporation (Passerat de Silans et al., 1989).

REFERENCES

Bird, R.B.; Stewart W.E.; and E.N. Lightfoot. 1965. *Transport Phenomena*. New York, New York: John Wiley & Sons. 780 pp.

Brutsaert, W. H. 1982. *Evaporation into the Atmosphere: Theory, History, and Applications*. London, England: D. Reidel Publishing Company. 299 pp.

Fritchen, L.J. and C.H.M. van Bavel. 1962. "Energy Balance Components of Evaporating Surfaces in Arid Lands." in *Journal of Geophysics Research*., Vol. 67, Baltimore, MD: American Geophysical Union. pp. 5179-5185.

MET (Multimedia Environmental Technology, Inc.). 1993. *Verification of A-TOUGH using Two-cell Mass Balance Model and VS2D*. Las Vegas, Nevada: Unpublished Report to Reynolds Electrical & Engineering Co.

MET. 1995. *User's Manual for A-TOUGH- An Atmospheric Interface Model based on V-TOUGH.* Newport Beach, California: Multimedia Environmental Technology, Inc. 59 pp.

Montazer, P.; Hammermeister, D.P.; and J. Ginanni. 1994. *A-TOUGH, A Multimedia Fluid-Flow/Energy-Transport Model for Fully-Coupled Atmospheric-Subsurface Interaction.* Proceedings of the Fifth Annual International Conference on High Level Radioactive Waste Management, Las Vegas, Nevada, May 22-26, 1994, American Nuclear Society, Inc., La Grange Park, Illinois. pp. 2333-2341.

Nitao, J.J. 1989. *V-TOUGH - An Enhanced Version of the TOUGH Code for the Thermal and Hydrologic Simulation of Large-Scale Problems in Nuclear Waste Isolation*. Berkeley, California: Lawrence Livermore National Laboratory, Draft 1.1, 24 pp.

Passerat de Silans, P.A.; Bruckler, L.; Thony, J.L.; and M. Vauclin. 1989. "Numerical Modeling of Coupled Heat and Water Flows During Drying in a Stratified Bare Soil - Comparison with Field Observations." *Journal of Hydrology*, Elsevier Science B.V., Amsterdam, Vol. 105, pp. 109-138.

Peixoto, J.P. and A.H. Oort. 1992. *Physics of Climate.* American Institute of Physics: New York, New York. 520 pp.

Penman, H.L. 1948. *Natural Evaporation from Open Water, Bare Soil and Grass*. Royal Society of London, Proceedings, Series A, No. 193. pp. 120-145.

Pruess, K. 1987. *TOUGH User's Guide*. LBL-20700. Berkeley, California: Lawrence Berkeley National Laboratories. Report LBNL-43134. 78 pp.

Pruess, K.; Oldenburg, C.; and G. Moridis. 1999. *TOUGH2 User's Guide*. LBNL-43134, Version 2.0. Berkeley, California: Lawrence Berkeley National Laboratories. 198 pp.

Stannard, D.I. 1993. *Comparison of Penman-Monteith, Shuttlewoth-Wallace, and Modified Priestly-Taylor Evapotranspiration Models for Wildland Vegetation in Semiarid Rangeland*. Water Resources Research, American Geophysical Union. Baltimore, MD. Vol. 29, No. 5, 1379 pp.

INTENTIONALLY LEFT BLANK

APPENDIX A FIGURES

INTENTIONALLY LEFT BLANK

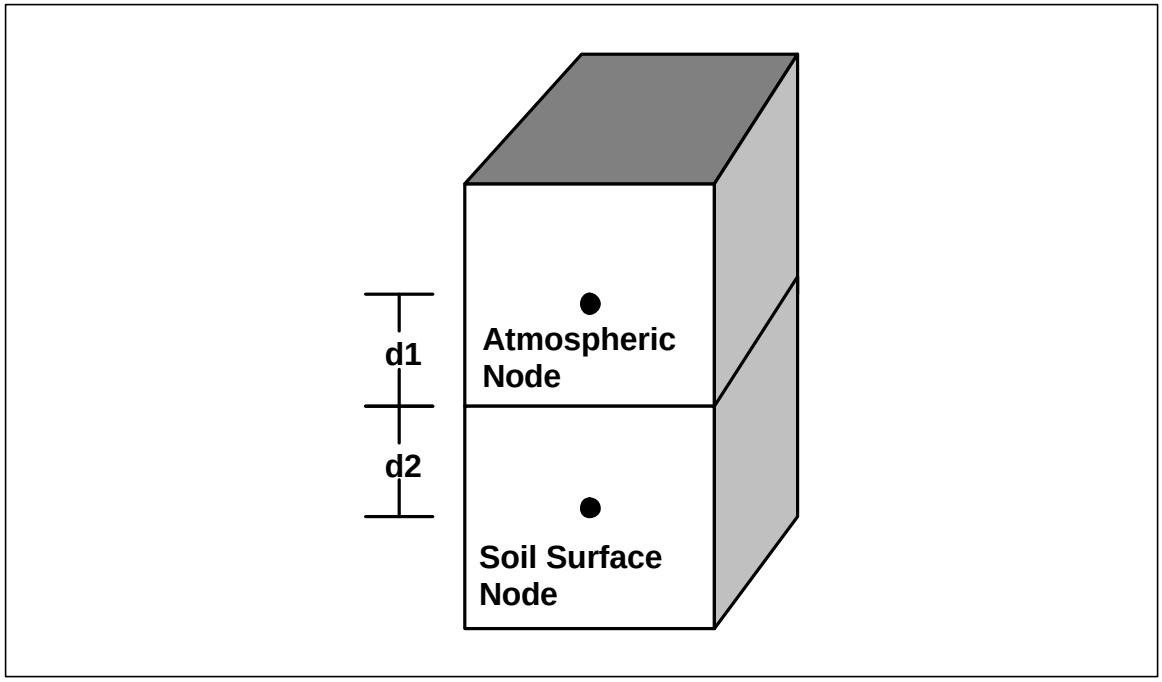

Figure A1
Schematic Diagram of Adjacent Atmospheric and Surface Nodes in A-TOUGH

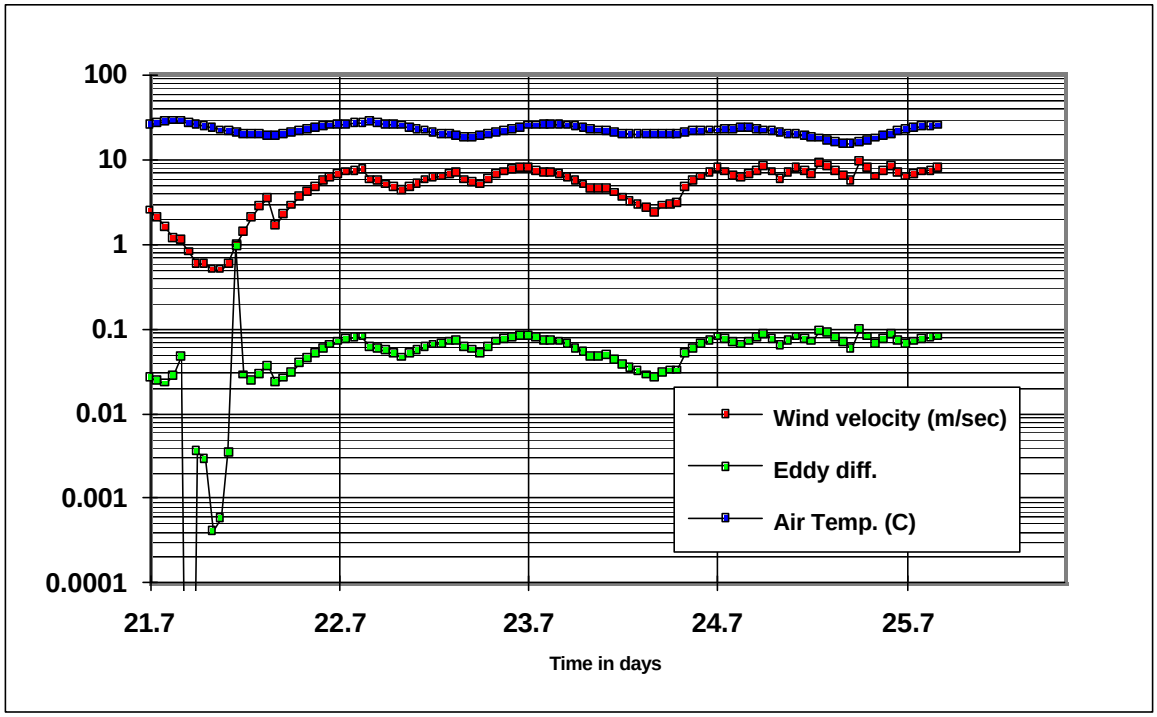

Figure A2
Calculated Eddy Diffusivity, Measured Air Temperature, and Wind Velocity in A-TOUGH2 Calibration Simulations

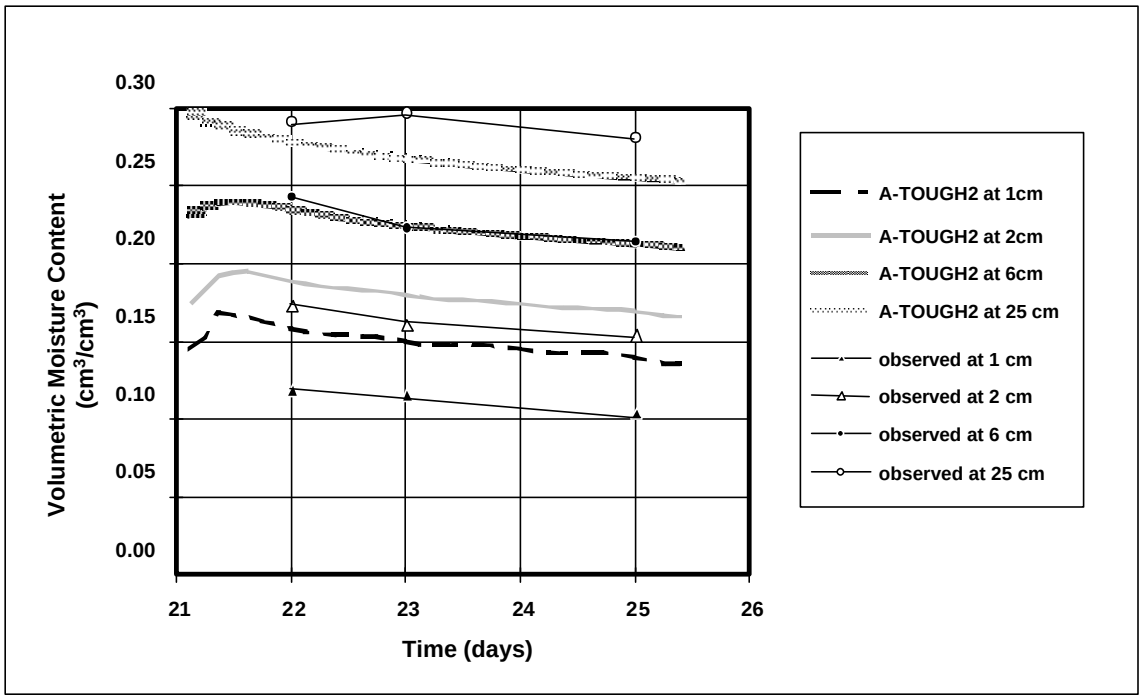

Figure A3
Comparison between Volumetric Moisture Content at Various Depths versus Time Observed by Passerat de Silans and Predicted by A-TOUGH2

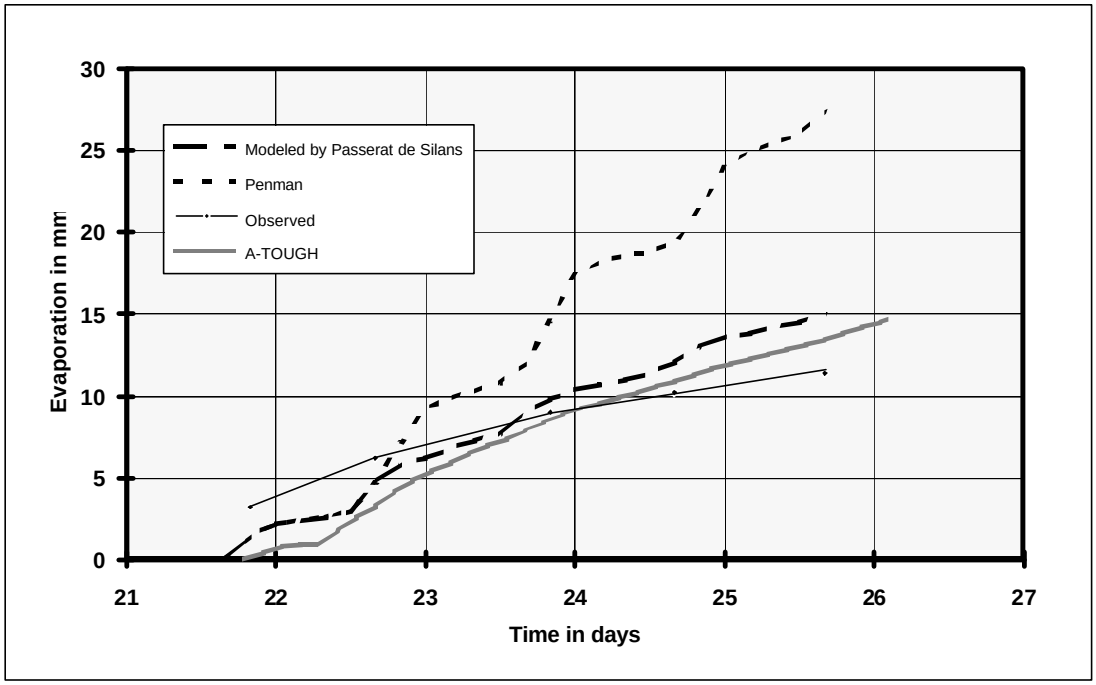

Figure A4
Cumulative Evaporation versus Time as Measured and Predicted by Passerat de Silans, Predicted by A-TOUGH, and Calculated by the Penman Method

APPENDIX A TABLES

INTENTIONALLY LEFT BLANK

Table A1
Summary of the Results of Two-Cell Verification Simulations

Run No.	D_{atm*} (m^2/s)	Input Variables: Ψsoil (m)	Input Variables: h(a) (fraction)	To (°K)	Ta (°K)	Analytical q_{evap} (kg/m^2-s)	A-TOUGH2 q_{evap} (kg/m^2-s)	sign	rel. err.
1	0.002	-100	0.1	278	278	-1.07E-05	-1.22E-05	1	-1.38E-01
2	0.002	-100	0.1	278	308	-4.18E-06	-5.45E-06	1	-3.03E-01
3	0.002	-100	0.1	308	278	-7.74E-05	-7.78E-05	1	-4.78E-03
4	0.002	-100	0.1	308	308	-7.09E-05	-7.10E-05	1	-2.18E-03
5	0.002	-100	1	278	278	9.18E-08	6.75E-10	1	9.93E-01
6	0.002	-100	1	278	308	6.72E-05	6.60E-05	1	1.85E-02
7	0.002	-100	1	308	278	-6.66E-05	-6.56E-05	1	1.54E-02
8	0.002	-100	1	308	308	5.57E-07	4.28E-07	1	2.33E-01
9	0.002	-1	0.1	278	278	-1.08E-05	-1.22E-05	1	-1.30E-01
10	0.002	-1	0.1	278	308	-4.47E-06	-5.47E-06	1	-2.80E-01
11	0.002	-1	0.1	308	278	-7.80E-05	-7.79E-05	1	1.13E-03
12	0.002	-1	0.1	308	308	-7.14E-05	-7.11E-05	1	4.25E-03
13	0.002	-1	1	278	278	9.22E-10	-1.69E-08	1	1.93E+01
14	0.002	-1	1	278	308	6.72E-05	6.60E-05	1	1.74E-02
15	0.002	-1	1	308	278	-6.71E-05	-6.57E-05	1	2.21E-02
16	0.002	-1	1	308	308	5.59E-09	3.34E-07	1	5.88E+01
17	0.2	-100	0.1	278	278	-1.07E-03	-1.22E-03	1	-1.38E-01
18	0.2	-100	0.1	278	308	-4.18E-04	-5.45E-04	1	-3.03E-01
19	0.2	-100	0.1	308	278	-7.74E-03	-7.78E-03	1	-4.78E-03
20	0.2	-100	0.1	308	308	-7.09E-03	-7.10E-03	1	-2.18E-03
21	0.2	-100	1	278	278	9.18E-06	6.75E-08	1	9.93E-01
22	0.2	-100	1	278	308	6.72E-03	6.60E-03	1	1.85E-02
23	0.2	-100	1	308	278	-6.66E-03	-6.56E-03	1	1.54E-02
24	0.2	-100	1	308	308	5.57E-05	4.28E-05	1	2.33E-01
25	0.2	-1	0.1	278	278	-1.08E-03	-1.22E-03	1	-1.30E-01
26	0.2	-1	0.1	278	308	-4.47E-04	-5.47E-04	1	-2.80E-01
27	0.2	-1	0.1	308	278	-7.80E-03	-7.79E-03	1	1.13E-03
28	0.2	-1	0.1	308	308	-7.14E-03	-7.11E-03	1	4.25E-03
29	0.2	-1	1	278	278	9.22E-08	-1.69E-06	1	1.93E+01
30	0.2	-1	1	278	308	6.72E-03	6.60E-03	1	1.74E-02
31	0.2	-1	1	308	278	-6.71E-03	-6.57E-03	1	2.21E-02
32	0.2	-1	1	308	308	5.59E-07	3.34E-05	1	5.88E+01

INTENTIONALLY LEFT BLANK

INTENTIONALLY LEFT BLANK

Table 1
Upper and Lower Boundary Conditions

Parameter	Atmospheric Boundary	Water Table Boundary
Absolute Pressure (Pa)	84510.758	92000
Temperature (°C)	18.7	32.4
Liquid Saturation (Fraction)	0	1

Table 2
Matrix Properties of the Stratigraphic Units

Unit	Permeability (m^2)	Porosity (Fraction)	Van Genuchten [a] (Pa^{-1})	Van Genuchten [b]	Residual Saturation (Fraction)	Satiated Saturation (Fraction)
tcwM1	3.86E-15	0.253	4.00E-05	0.47	0.07	1
tcwM2	2.74E-19	0.082	1.81E-05	0.241	0.19	1
tcwM3	9.23E-17	0.203	3.44E-06	0.398	0.31	1
ptnM1	9.90E-13	0.387	1.01E-05	0.176	0.23	1
ptnM2	2.65E-12	0.439	1.60E-04	0.326	0.16	1
ptnM3	1.23E-13	0.254	5.58E-06	0.397	0.08	1
ptnM4	7.86E-14	0.411	1.53E-04	0.225	0.14	1
ptnM5	7.00E-14	0.499	5.27E-05	0.323	0.06	1
ptnM6	2.21E-13	0.492	2.49E-04	0.285	0.05	1
tswM1	6.32E-17	0.053	3.61E-05	0.303	0.22	1
tswM2	5.83E-16	0.157	3.61E-05	0.333	0.07	1
tswM3	3.08E-17	0.154	2.13E-05	0.298	0.12	1
tswM4	4.07E-18	0.11	3.86E-06	0.291	0.19	1
tswM5	3.04E-17	0.131	6.44E-06	0.236	0.12	1
tswM6	5.71E-18	0.112	3.55E-06	0.38	0.18	1
tswM7	4.49E-18	0.094	5.33E-06	0.425	0.25	1
tswM8	4.53E-18	0.037	6.94E-06	0.324	0.44	1
tswM9	5.46E-17	0.173	2.29E-05	0.38	0.29	1
chM1z	1.96E-19	0.288	2.68E-07	0.316	0.33	1
chM1v	9.90E-13	0.273	1.43E-05	0.35	0.03	1
chM2v	9.27E-14	0.345	5.13E-05	0.299	0.07	1
chM3v	9.27E-14	0.345	5.13E-05	0.299	0.07	1
chM4v	9.27E-14	0.345	5.13E-05	0.299	0.07	1
chM5v	9.27E-14	0.345	5.13E-05	0.299	0.07	1
chM2z	6.07E-18	0.331	3.47E-06	0.244	0.28	1
chM3z	6.07E-18	0.331	3.47E-06	0.244	0.28	1
chM4z	6.07E-18	0.331	3.47E-06	0.244	0.28	1
chM5z	6.07E-18	0.331	3.47E-06	0.244	0.28	1
chM6	4.23E-19	0.266	3.38E-07	0.51	0.37	1
ppM4	4.28E-18	0.325	1.51E-07	0.676	0.28	1
ppM3	2.56E-14	0.303	2.60E-05	0.363	0.1	1
ppM2	1.57E-16	0.263	2.67E-06	0.369	0.18	1
ppM1	6.40E-17	0.28	1.14E-06	0.409	0.3	1
bfM3	2.34E-14	0.115	4.48E-06	0.481	0.11	1
bfM2	2.51E-17	0.259	1.54E-07	0.569	0.18	1

Source: DOE (2000a)

Table 3
Fracture Properties of the Stratigraphic Units

Unit	Perme-ability (m^2)	Porosity (Fraction)	Van Genuch-ten a (Pa^{-1})	Van Genuch-ten b	Residual Saturation (Fraction)	Satiated Saturation (Fraction)	Active Fracture Parameter	Frequency (1/m)	Fracture to Matrix Area (m^2/m^3)
tswF1	2.41E-12	0.028	3.15E-03	0.627	0.01	1	0.30	0.92	1.56
tswF2	1.00E-10	0.02	2.13E-03	0.613	0.01	1	0.30	1.91	13.39
tswF3	5.42E-12	0.015	1.26E-03	0.607	0.01	1	0.30	2.79	3.77
ptnF1	1.86E-12	0.011	1.68E-03	0.58	0.01	1	0.09	0.67	1.00
ptnF2	2.00E-11	0.012	7.68E-04	0.58	0.01	1	0.09	0.46	1.41
ptnF3	2.60E-13	0.0025	9.23E-04	0.61	0.01	1	0.09	0.57	1.75
ptnF4	4.67E-13	0.012	3.37E-03	0.623	0.01	1	0.09	0.46	0.34
ptnF5	7.03E-13	0.0062	6.33E-04	0.644	0.01	1	0.09	0.52	1.09
ptnF6	4.44E-13	0.0036	2.79E-04	0.552	0.01	1	0.09	0.97	3.56
tswF1	3.21E-11	0.0055	2.49E-04	0.566	0.01	1	0.06	2.17	3.86
tswF2	1.26E-12	0.0095	1.27E-03	0.608	0.01	1	0.41	1.12	3.21
tswF3	5.50E-13	0.0066	1.46E-03	0.608	0.01	1	0.41	0.81	4.44
tswF4	2.76E-13	0.01	5.16E-04	0.608	0.01	1	0.41	4.32	13.54
tswF5	1.29E-12	0.011	7.39E-04	0.611	0.01	1	0.41	3.16	9.68
tswF6	9.91E-13	0.015	7.84E-04	0.61	0.01	1	0.41	4.02	12.31
tswF7	9.91E-13	0.015	7.84E-04	0.61	0.01	1	0.41	4.02	12.31
tswF8	5.92E-13	0.012	4.87E-04	0.612	0.01	1	0.41	4.36	13.34
tswF9	4.57E-13	0.0046	9.63E-04	0.634	0.01	1	0.41	0.96	2.95
chFz	3.40E-13	0.0002	1.43E-03	0.631	0.01	1	0.10	0.04	0.11
chFv	1.84E-12	0.0007	1.09E-03	0.624	0.01	1	0.13	0.10	0.30
chF2v	2.89E-13	0.0009	5.18E-04	0.628	0.01	1	0.13	0.14	0.43
chF3v	2.89E-13	0.0009	5.18E-04	0.628	0.01	1	0.13	0.14	0.43
chF4v	2.89E-13	0.0009	5.18E-04	0.628	0.01	1	0.13	0.14	0.43
chF5v	2.89E-13	0.0009	5.18E-04	0.628	0.01	1	0.13	0.14	0.43
chF2z	3.12E-14	0.0004	4.88E-04	0.598	0.01	1	0.10	0.14	0.43
chF3z	3.12E-14	0.0004	4.88E-04	0.598	0.01	1	0.10	0.14	0.43
chF4z	3.12E-14	0.0004	4.88E-04	0.598	0.01	1	0.10	0.14	0.43
chF5z	3.12E-14	0.0004	4.88E-04	0.598	0.01	1	0.10	0.14	0.43
chF6	1.67E-14	0.0002	7.49E-04	0.604	0.01	1	0.10	0.04	0.11
ppF4	3.84E-14	0.0004	5.72E-04	0.627	0.01	1	0.10	0.14	0.43
ppF3	7.60E-12	0.0011	8.73E-04	0.655	0.01	1	0.46	0.20	0.61
ppF2	1.38E-13	0.0011	1.21E-03	0.606	0.01	1	0.46	0.20	0.61
ppF1	1.12E-13	0.0004	5.33E-04	0.622	0.01	1	0.10	0.14	0.43
bfF3	4.08E-13	0.0011	9.95E-04	0.624	0.01	1	0.46	0.20	0.61
bfF2	1.30E-14	0.0004	5.42E-04	0.608	0.01	1	0.10	0.14	0.43

Source: DOE (2000a)

Table 4
Mean Thermal Properties of the Stratigraphic Units

Model Layer	Rock Grain Density (Kg/m^3)	Rock Grain Specific Heat (J/Kg K)	Dry Conductivity (W/m K)	Wet Conductivity (W/m K)
tcwM1	2550	823	1.6	2
tcwM2	2510	851	1.24	1.81
tcwM3	2470	857	0.54	0.98
ptnM1	2380	1040	0.5	1.07
ptnM2	2340	1080	0.35	0.5
ptnM3	2400	849	0.44	0.97
ptnM4	2370	1020	0.46	1.02
ptnM5	2260	1330	0.35	0.82
ptnM6	2370	1220	0.23	0.67
tswM1	2510	834	0.37	1
tswM2	2550	866	1.06	1.62
tswM3	2510	882	0.79	1.68
tswM4	2530	948	1.56	2.33
tswM5	2540	900	1.2	2.02
tswM6	2560	865	1.42	1.84
tswM7	2560	865	1.42	1.84
tswM8	2360	984	1.69	2.08
tswM9	2360	984	1.69	2.08
chM1z	2310	1060	0.7	1.31
chM1v	2310	1060	0.7	1.31
chM2v	2240	1200	0.58	1.17
chM3v	2240	1200	0.58	1.17
chM4v	2240	1200	0.58	1.17
chM5v	2240	1200	0.58	1.17
chM2z	2350	1150	0.61	1.2
chM3z	2350	1150	0.61	1.2
chM4z	2350	1150	0.61	1.2
chM5z	2350	1150	0.61	1.2
chM6	2440	1170	0.73	1.35
ppM4	2410	577	0.62	1.21
ppM3	2580	841	0.66	1.26
ppM2	2580	841	0.66	1.26
ppM1	2470	635	0.72	1.33
bfM3	2570	763	1.41	1.83
bfM2	2410	633	0.74	1.36

Source: DOE (2000c)

Table 5
Initial Drift Design Parameters

Feature	Value
Ventilation drift diameter**	8.5 m
Waste package borehole/drift diameter**	2.5 and 5.5 m
Waste package outer diameter	1.67 m
Diameter of rubble backfill to fill the drifts and shafts*	0.02 m
Waste package thermal conductivity*	14.42 W/m-K
Waste package density*	8189.2 kg/m 3
Waste package specific heat*	488.86 J/kg-K
Rubble backfill intrinsic permeability**	$1.x10^{-5}$ m^2
Rubble backfill porosity*	0.41
Rubble backfill grain density*	2700 kg/m 3
Rubble backfill residual liquid saturation*	0.024
Rubble backfill alpha (van Genuchten)*	$2.7523x10^{-4}$ Pa^{-1}
Rubble backfill n (van Genuchten)*	2.0
Rubble backfill specific heat**	795.492 J/kg-K
Rubble backfill thermal conductivity**	0.33 W/m-K

Source: DOE (2000c)

NOTES: * Not used for simulations in this report
** Modified after DOE (2000c)

Table 6
Heat Load

Time (years)	Power (W/m)
0	1547.300
1	1500.726
5	1360.541
10	1227.783
15	1117.615
20	1024.777
26	926.678
30	868.190
40	746.418
50	648.938
60	570.644
70	507.669
80	455.989
90	414.057
100	379.398
125	328.182
150	276.812
200	229.774
250	201.613
300	181.962

Source: DOE (2000c)

Table 7
Summary of Preliminary Simulation Results

Simulation File Number (Mesh No.)	Figure Number	TSw Fracture and Matrix Permeability			Infiltration		Grid Type				Spacing and Heat Sources									
		Mean	Upper Bound	Lower Bound	Mean	Upper Bound	Simulation No.	Mesh Type	Grid size (Columns/Rows/Slices)	Dimensions (m) (Width/ Depth/ Thickness)	Starting Time for Heat-Load Application	Drift diameter	Number of drifts	Drift Spacing	No. of heaters between drifts	Fraction of Full Load	Total No. of Heaters	Acreage Requirement	Time (yr.) for Peak Temperature	Peak Temperature (C)
DFM02 (4) (Steady State)	NP	X				X	1	Fine	40/ 24/1	400/540/ 10	0	NA	NA	NA	NA	NA	NA	NA	NA	NA
DFMWH02 (4)	NP	X				X	2	Fine	40/ 24/1	400/540/ 10	0	8.5	10	70	6	0.03	24	NA	NA	35
DFMWH03 (4)	NP	X				X	3	Fine	40/ 24/1	400/540/ 10	0	8.5	10	70	6	0.3	24	830	>4	> 100
DFMWH04 (4)	NP	X				X	4	Fine	40/ 24/1	400/540/ 10	0	8.5	10	70	4	0.2	20	1250	>5	> 100
DFMWH05 (4)	NP	X				X	5	Fine	40/ 24/1	400/540/ 10	0	8.5	10	70	4	0.8	20	312	>1	> 100
DFMWH06 (4)	NP	TSw x 10^3				X	6	Fine	40/ 24/1	400/540/ 10	0	8.5	10	70	4	0.8	20	312	<1	>94
DFMWH07 (4)	NP	TSw x 10^3				X	7	Fine	40/ 24/1	400/540/ 10	0	8.5	10	70	4	0.8	20	312	<1	>90
FMWH0250 (4)	12-15	X				X	8	Fine	40/ 24/1	400/540/ 10	50	8.5	10	70	6	0.3	24	833	62.5	> 100
DFM150H (4)	16-19	X				X	9	Fine	40/ 24/1	400/540/ 10	150	8.5	10	70	6	0.3	24	833	420	>82
DFM300H (4)	20-21	X				X	10	Fine	40/ 24/1	400/540/ 10	300	8.5	10	70	6	0.3	24	833	420	>27
D300TnFL (4)	NP	X				X	11	Fine	40/ 24/1	400/540/ 10	300	8.5	10	70	6	0.12	24	2083	> 720	<42
DFM310FL (4)	NP	X				X	12	Fine	40/ 24/1	400/540/ 10	300	8.5	10	70	6	1.2	24	208	< 301	> 120
2H1D300 (4)	NP	X				X	13	Fine	40/ 24/1	400/540/ 10	250	8.5	22	30	2	1.0	20	< 250	720	<90
2H1D300H (4)	22-24	X				X	14	Fine	40/ 24/1	400/540/ 10	250	8.5	22	30	2	0.5	20	< 500	720	<50

NOTES: X indicates parameter/case simulated; NA = not applicable; NP = graphic results are not presented in this report

*In the coarse mesh, the drift nodes vary from 20 to 70 m wide and are all 22.5 m high. Therefore, they represent multiple ventilation drifts.